CCDC57 COOPERATES WITH MICROTUBULES AND MICROCEPHALY PROTEIN CEP63 AND REGULATES CENTRIOLE DUPLICATION AND MITOTIC PROGRESSION

by

Hazal Kübra Gürkaşlar

Thesis Submitted to the
Graduate School of Science and Engineering
in Fulfillment of the Requirements for the Degree of

Master of Science

at

Molecular Biology and Genetics

January 6, 2020

Koç University
Graduate School of Sciences and Engineering

This is to certify that I have examined this copy of master's thesis by

Hazal Kübra Gürkaşlar

and have found that it is complete and satisfactory in all respects,

and that any and all revisions required by the final

examining committee have been made.

Committee Members:

Assistant Prof. Dr. Elif Nur Fırat Karalar (Advisor, Koc University)

Assistant Prof. Dr. Ayşe Koca Çaydaşı (Koc University)

Associate Prof. Dr. İbrahim Yaman (Boğaziçi University)

Date: JANUARY 6, 2020

ABSTRACT

Centrosomes play critical roles in diverse cellular processes ranging from cell division to cellular signaling. At the core of the centrosomes are two centrioles, which duplicate only once per cell cycle and this duplication cycle is tightly regulated. Accordingly, their deregulation causes diseases such as cancer and developmental disorders like primary microcephaly. Complete understanding of the mechanisms that regulate centrosome biogenesis and function is required to elucidate the disease mechanisms. In this study, we identified a new centrosome protein CCDC57, which also localizes and binds to centriolar satellites and microtubules. Proximity-labeling and interaction studies showed that CCDC57 forms a complex with Cep63, centriolar satellites and microtubules. Importantly, characterization of CCDC57 deletion mutants revealed that its N-terminal 1-502 amino acid region mediated its centrosomal localization and interactions, whereas the C-terminal 606-916 amino acid region mediated its localization and binding to microtubules. Loss of CCDC57 causes defects in canonical centriole duplication and centriole amplification, and results in a failure to localize microcephaly-associated proteins Cep63 and Cep152 to the centriole during initiation of centriole duplication. Additionally, CCDC57 depletion resulted in prolonged mitosis, increased apoptosis and a higher ratio of mitotic defects such as misaligned chromosomes and multipolar spindles. Together, our results identify CCDC57 as dual regulator of the Cep63 centriole duplication module and microtubule-mediated mitotic processes and provide new mechanistic insight into defects underlying cancer and primary microcephaly.

ÖZET

Centrozomlar, hücre bölünmesinden hücresel sinyal iletimine kadar çeşitli süreçlerde kritik roller oynarlar. Centrozomların temel yapısında, her hücre döngüsünde sadece bir kez çoğaltılan ve bu çoğaltma döngüsü sıkı bir şekilde düzenlenmiş iki sentriyol vardır. Bununla ilişkili olarak, regülasyonlarındaki bozukluklar kanser gibi hastalıklara ve birincil mikrosefali gibi gelişimsel bozukluklara neden olur. Hastalık mekanizmalarını aydınlatmak için sentrozom biyogenezini ve fonksiyonunu düzenleyen mekanizmaların tam olarak anlaşılması gerekmektedir. Bu çalışmada, ayrıca sentriyolar uydu proteinleri ile birlikte localize olan, mikrotübüllere bağlanan ve yeni bir sentrozom proteini olan CCDC57 tanımladık. Yakınlık temelli etiketleme ve etkileşim çalışmaları, CCDC57'nin Cep63, sentriolar uydular ve mikrotübüller ile bir kompleks oluşturduğunu göstermiştir. Önemli olarak, CCDC57 parça mutantlarının karakterizasyonu, N-terminal 1-502 amino asit bölgesinin, sentrozomal konumlanmasına ve etkileşimlerine aracılık ederken, C-terminal 606-916 amino asit bölgesinin, mikrotübüllere bağlanmasına aracılık ettiğini ortaya çıkarmıştır. CCDC57'nin susturulması kanonik sentriyol eşlenmesinde ve sentriyol çoğalmasında hatalara neden olur ve sentriyol eşlenmesinin başlaması sırasında mikrosefali ile ilişkili protein Cep63 ve Cep152'nin sentriyole konumlanması başarısızlıkla sonuçlanır. Ek olarak, CCDC57'nin susturulması daha uzun süren mitoz bölünme, artan apoptoz, yanlış hizalanmış kromozomlar ve çok kutuplu iğler gibi mitotik kusurlar ile sonuçlanmıştır. Tüm sonuçlar birlikte, CCDC57'yi Cep63 sentriole çoğaltma modülünün ve mikrotübül aracılı mitotik süreçlerin ikili düzenleyicisi olarak tanımlar ve kanser ve primer mikrosefali hastalıklarının altında yatan sorunlara yeni mekanik bir bakış sağlar.

ACKNOWLEDGEMENTS

My adventure was started in 2011 in Boğaziçi university. I made the decision to study Molecular Biology and Genetics while I was at high school because cancer tragically took away my close friend, Çağatay Budak. First, I would like to thank you for your good heart because you are the reason for why I am here. It took some time to adapt to the school because I was building a new life in Istanbul at the same time. During that time, I met Ebru Doğan. She has always supported me and help me. Our friendship was a breakpoint for mylife in Istanbul. Thank you Ebru, you are my best, and I love you so much. For my academic life, I started to work in Molecular Toxicology and Cancer research laboratory since the summer of 2014 when I was a bachelor, and I have always been happy to be in the lab. My first PI, Ibrahim Yaman has always supported me. Although I did not have a good GPA, he gave that opportunity to me to work with him. In this lab I improved myself in different aspects and I met very good people. First, I would like to thank our sister lab, CSL, members; Ali İşbilir, Burçin Duan Şahbaz, Tolga Aslan, Tuncay Şeker, Aida Shahraki and İzzet Akiva. We shared everything with them, and we were a good team. Our second sister lab was AKİL. I have wonderful memories for that time. Aybüke Garibcan, Açelya Yılmazer, Emre Kırgın, Mesut Berber, Orhun Külekçi, İlke Süder and Alper Çevirgel; all you are my precious. I always miss you and our good times, and we have dealt with every problem together. Thank you for everything. I could not survive without your support and love. Other thanks go to “Destek Hattı” members. It is a mixed group from different labs in Boğaziçi university. Emir Erkol, Selif Eski, Gizem Olay Artık, Ulduz Sophi Afshar, Duygu Yeşildağ, Anna, Bilal Başdağ, Ecem Çayıroğlu, and Harun Öztürk. You are the best supportive group in any time and any condition. Your friendship is very valuable for me. You are one of the reasons for my best time in life. I love you so much, and thanks for everything. Also, I would like to thank my professors in Boğaziçi University. The best one is always Ibrahim Yaman, and then Arzu Çelik-Fuss, Necla Birgül-İyison, Stefan Fuss, Nesrin Özören, Tolga Emre and Umut Şahin; thank you for every single word that you taught me, and again for your friendly attitudes. The biggest thank goes to Yaman Lab members; Zeynep Özcan, Ayşin Demirkol Akpınar, Gizem Gül, Beren Aylan and Can Gürkaşlar. The first person who I met in the lab was Ayşin Demirkol Akpınar. I learnt to much about academic life from her. Whenever I had a trouble, she helped me to solve

it. She was the first who taught me to use micropippete. Even though she is far away now, she will always be my sister. Thank you for everything. You will always be the best lab in the world. I also want to thank all MBG department in Boğaziçi University. I am very lucky to be there and to meet you. I wish all the best for you.

After my adventure in Boğaziçi university, I started to work with Elif Nur Fırat Karalar in Cytoskeleton Research Laboratory in Koç university for my masters study. It was not easy to adapt a new environment, so I needed someone to share my feelings. After a while, I started to share everything with my PI, Elif Hoca, and her support is indispensable for me in Koç university. From the beginning to the end, she always trusts me, and she offered me every opportunity. Thank you hocam for everything, I feel very lucky to be here. Also, I would like to thank my both labmate and roomie, Ezgi Odabaşı for her helps and patience. The newest lab memberJovana Deretic is another person, I would like to thank. Even though we do not spend too much time together, but we shared lots of good times. Efraim Culfa is our former lab member and I continued his project. He was always very kind and helpful to me, so thank you very much. Lastly, Fatmanur Tiryaki, Umut Batman, Dila Gülensoy and Ebru Topçu, after you started the lab, you create a good and energic lab environment, so I also want to thank you for these. I really love you. Mehmet Akdağ, you are my best in Koç university because I could not survive here without your support. I also want to thank Nazlı Ezgi Özkan Küçük, İbrahim Oğuz, Şevval Bilgiç, Batu Toledo for your good friendship, and all MBGE department. I'd also like to thank my thesis commitee members İbrahim Yaman and Ayşe Koca Çaydaşı for accepting to be my juries.

At the end, biggest thank goes to my big family. Serap Gürkaşlar and Hasan Gürkaşlar, you are my second family now, and I am very happy to be a member of your family. My mother, Çiğdem Zırhlıoğlu will always be the best for my life. Words are insufficient to explain my love for her. I also would like to thank my father, Gürol Zırhlıoğlu. Thank you to force me to study here. This one of the best things that I experienced in my life. My dearest sister, İrem Gülçin Zırhlıoğlu, I love you so much and you will always be my everything. The last person I would like to thank is Can Gürkaşlar. You have been always with me during this process and now, we share our lifes. I love you too much my darling, I am lucky to be with you. All of you are my LOVE!!!

Table of Contents

List of Figures

NOMENCLATURE

GAMMA TURC	Gamma Tubulin Ring Complex
CCDC	Coiled coil domain containing
DEUP1	Deuterosome Assembly Protein 1
PCM	Pericentriolar Material
C-NAP1	Centrosomal Nek2 Associated Protein
LRRC45	Leucine Rich Repeat Containing 45
MTOC	Microtubule Organizing Center
CEP	Centrosomal Protein
SCLT1	Sodium Channel and Clathrin Linker 1
FBF1	Fas Binding Factor 1
ODF2	Outer Dense Fibers of Sperm Tails 2
TCHP	Trichoplein Keratin Filament Binding
CP110	Centriolar Coiled-Coil Protein 110
PCNT	Pericentrin
CDK5RAP2	CDK5 Regulatory Subunit Associated Protein 2
PLK	Polo Like Kinase
PCM-1	Pericentriolar Material 1
TZ	Transition Zone

NPHP	Nephrocystin
MKS	Meckel-Gruber Syndrome
BBS	Bardet-Biedl Sydrome
IFT	Intraflagellar Transport
RTK	Receptor Tyrosine Kinase
CV	Ciliary Vesicle
GEF	Guanine Nucleotide Exchange Factor
ALI	Air Liquid Interphase
CTL	Cytotoxic T Lymphocyte
GFP	Green Fluorescent Protein
NGS	Next Generation Sequencing
RD	Retinal Degeneration
HELA	Henrietta Lacks
ciRNA	Circular RNA
PEG	Polyethylene Glycol
BIRA	Biotin Protein Ligase
BIRA*	Promiscuous Biotin Protein Ligase
DNA	Deoxyribonucleic Acid
SIRNA	Short interference RNA

RNA	Ribonucleic Acid
RPE1	Retinal Pigment Epithelial 1 Cells
COP1	Coat Protein Complex 1
KIF	Kinesins Gene Family
HSAV1	Salvador
MST2	Mammalian Sterile 20-Like Kinase 2
NEK2	Never in Mitosis A-Related Kinase 2
GAPDH	Glyceraldehyde 3-Phosphate Dehydrogenase
CPAP	Centrosomal P4.1-Associated Protein
HEK293T	Human Embryonic Kidney 293 T antigen cells
BIOID	Proximity-Dependent Biotin Identification
CNN	Centrosomin
SPD-5	Spindle Defective Protein 5
MCHP	Primary Autosomal Recessive Microcephaly
ZNF335	Zinc Finger Protein 335

1 INTRODUCTION

The German biologist Theodor Boveri discovered centrosome more than hundred years ago, and he realized that centrosome is important for proper chromosome segregation during cell cycle. He gave the information about centrosome localization and he had stated that centrosome localized in the middle of newly formed cells (Scheer 2014).

Today, it is known that centrosome is an organelle which do not have membrane, and they are classified as the main microtubule organizing center (MTOC) in animal cells. Centrosome has different functions which are cell polarity, trafficking in the cell and cellular movement. During mitotic cell division, the centrosome is responsible for microtubule nucleation and bipolar spindle formation to separate chromosomes uniformly into daughter cells. Each centrosome has to centrioles, and it is surrounded by pericentriolar material (PCM). In vertebrates, there is another structure called as centriolar satellites. They are small and electron dense structures concentrate around the centrosome and distribute throughout the cell with the help of microtubules (Bettencourt-Dias and Glover 2007, Barenz, Mayilo et al. 2011).

Centrioles are evolutionary conserved microtubule-based structure which has nine fold symmetry and are 200nm in diameter and 500nm in length (Bornens 2002). They are perpendicular to each other and their proximal ends are enclosed by the pericentriolar material in the time they grow from their distal ends. The two centrioles differ from each other structurally and biochemically. The older centriole is called as “mother centriole”, and it has extra protein complexes known as distal- and subdistal appendages. However, the other centriole does not have such structure and it is named as “daughter centriole” (Winey and O'Toole 2014). One of the most important role of the centrosome is the cilium formation, and distal appendage proteins lead this process by anchoring the centrosome to the cell membrane. The formation of cilium takes place through the hierarchical arrangement of distal appendage proteins (Tanos, Yang et al. 2013). Additionally, subdistal appendage proteins are responsible for

microtubule nucleation in interphase cells. Sub-distal appendage proteins also form that structures by coming together with an order (Huang, Xia et al. 2017).

Centrioles recruit the pericentriolar material proteins to form the centrosome. Pericentriolar material is not amorphous, instead it has a highly regulated architecture, as revealed by their analysis using superresolution microscopy. Gamma-tubulin ring complexes localize to the PCM and functions in nucleating microtubules from there (Kollman, Merdes et al. 2011). There are many proteomics studies that have revealed the components of pericentriolar material of various cells and species. High resolution microscopy studies for known PCM proteins showed spatial organization of these proteins in concentric rings (Sonnen, Schermelleh et al. 2012, Bauer, Cubizolles et al. 2016).

Like DNA, centrioles replicate once and only once in each cell division to distribute duplicated DNA into daughter cells equally (Nigg 2007). Centriole number must be tightly regulated because any defect in centriole duplication induces cancer progression through aneuploidy and stimulating invasive behavior. Inducible expression of a key kinase for centriole duplication in mouse causes formation of extra centrioles, which results in spontaneous tumor formation, providing further support that extra centrosomes cause cancer (Levine, Bakker et al. 2017). Given their tight association with cancer, we aimed to mechanistically dissect the canonical centriole duplication pathway in mammalian cells. Although evolutionariliy conserved proteins of the pathway have been identified in different species, there is little information on how vertebrates evolved to accommodate their higher complexity during development and differentiation. To this end, we focused on identifying new centriolar satellite components that function in centriole duplication. Through functional and biochemical characterization experiments, we identified CCDC57 as a dual regulator of centriole duplication and mitosis and defined the centriolar recruitment of Cep63-Cep152 duplication module and regulation of microtubule dynamics as the mechanism underlying its functions. Chapter two contains a thorough literature review mainly about centrosome, cilium, centriole duplication, centriolar satellites and cell division. Chapter three covers our findings on CCDC57, which we submitted as a research article

and are currently working on the revisions. The last chapter consists of material and methods.

2 LITERATURE REVIEW

2.1 CENTROSOME

Centrosome is the main microtubule nucleation factor in animal cells. In an interphase cell, microtubules radiating from the centrosome which has several functions such as trafficking, cell polarity and cell movement. In a dividing cell, the centrosome goes to the poles of the cell and forms spindle microtubules to distribute DNA to newly formed cells equally.

Centrosome is composed of two centrioles which are surrounded by pericentriolar material (PCM). In vertebrates, there are electron dense proteins called as centriolar satellites and they localize around centrosome by binding to microtubules (Barenz et al., 2011; Tollenaere et al., 2015). Microtubules form the centrioles which has 250 nm width and 500nm height. Importantly, the centriole structure is highly conserved in different species, and it is nine-fold symmetric ring. Centrioles are perpendicular to each other from their proximal ends where they are surrounded by pericentriolar material and the distal ends elongate from their proximal parts. Fine basic differences between the two centrioles of a centrosome is additionally an obvious property, so two centrioles are named differentially. Older one with its distal- and subdistal-appendages is called as “mother centriole” while the other “daughter centriole” does not have these extensions (Winey and O'Toole 2014).

Centrioles capture certain proteins wtih an order to form pericentriolar material which works as a microtubule nucleation region and PCM cooparates with sub-distal appendeges during microtubule formation (Woodruff, Wueseke et al. 2014) and (Gorgidze and Vorobjev 1995). Gamma tubulin ring complex (γ-TURC) has a tendency to interact with alpha- and beta- tubulins in PCM and it is responsible for microtubule nucleation process (Kollman, Merdes et al. 2011). In figure 2.1, schematic representation of the structure of centrioles is shown.

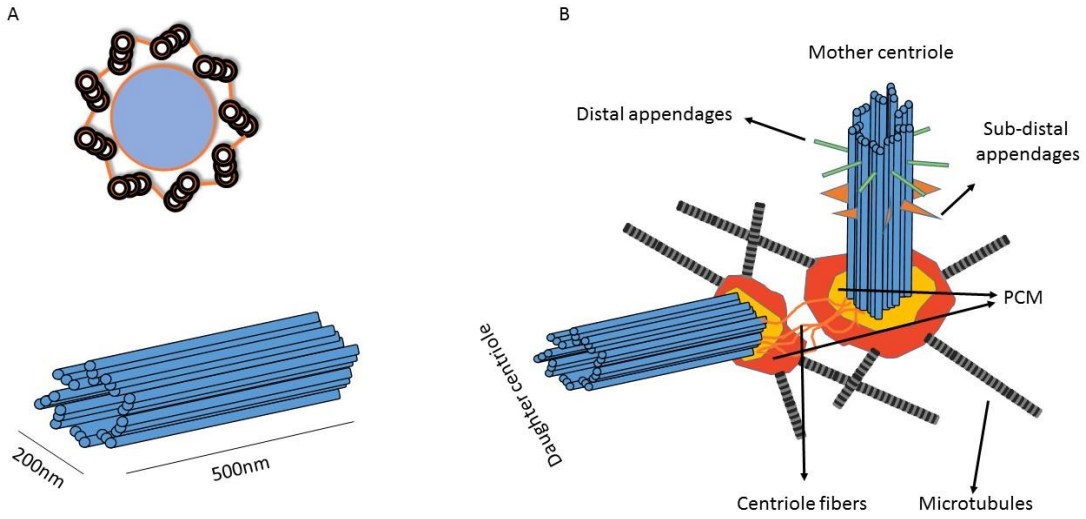

Figure 2.1 Structure of Centrosome A) The centrioles with 500 nm height and 200nm width are the main structures for centrosome and they have 9-fold symmetric shape. B) Mother centriole has the appendage proteins which have distal and sub-distal localization on the distal end of the centriole, but daughter centriole does not have those proteins. PCM proteins are concentrated around the centrioles, mainly mother centriole, and PCM takes role during microtubule nucleation. Centriole fibers connect two centrioles to each other.

2.1.1 CENTRIOLES

Centrioles are big structures which have 200nm in width and 500nm in heigth because they also collect certain proteins and form a complex. Microtubules are the building block of the centrioles and they have lots of post-translational modifications such as detyrosination, acetylation, and glutamylation. All these modifications make the centrosomes more stable and they have ressistance against cold and depolymerizing reagents like nocodazole (Janke and Bulinski 2011). Centrioles are composed of 9-fold symmetric triplet microtubules and every fold contains three microtubules which are A, B, and C tubules. While A tubule is composed of 13 protofilaments, 10 protofilaments constitute B and C tubules. These tubules have a distinct organization to be sure that B and C tubules complete the number of their protofilaments to 13 by sharing extra 3 protofilaments (Guichard, Hachet et al. 2013). Centrioles have the nine fold symmetric structure in different species, but they differ in terms of their microtubule arrangement. For example, centriole structure of *Drosophila melanogaster* and *Caenorhabditis elegans* is different from the mammalians and they

have two microtubules and single microtubule in every fold respectively (Bettencourt-Dias and Glover 2007).

The ends of the centrioles are different in their composition and structure. The part of the centriole associated with the PCM1 is called the “proximal end” and the other end of the centriole is called as “distal end” (Li, Fernandez et al. 2012). A subset of proteins including C-NAP1, Rootletin, Cep68 and LRRC45 are responsible to link the two centrioles to each other and they are known as linker proteins (Fry, Mayor et al. 1998), (Yang, Liu et al. 2002) and (He, Huang et al. 2013). To ensure that interphase cells have only one microtubule organizing center, these linker proteins create cohesion and keep the centrioles together (Nigg and Stearns 2011). As cells enter to S and G2 phases, the linker proteins are degraded after Nek2-mediated phosphorylation . The new procentrioles are translocated to the spindle poles with kinesin motor proteins during mitosis (Tanenbaum and Medema 2010). If centrioles are separated from each other in interphase cells, it is termed as “premature centrosome splitting” (Nigg 2007). This phenotype is observed because of the mutations on the linker proteins, and mutations of C-Nap1 causes Seckel like syndrome(Floriot, Vesque et al. 2015).

Two centrioles do not look like the same because mother centriole has certain protein complexes on its distal end and these complexes are called as distal- and subdistal appendages, but they are not found on the daughter centriole. Composition of the distal appendages contains various proteins which are CEP89, CEP83, CEP164, SCLT1 and FBF1 (Tanos, Yang et al. 2013) while subdistal appendage proteins which are ODF2, CCDC68, CCDC120, TCHP,CEP170 and NINEIN are assembled in a similar hierarchical manner like distal appendage proteins (Huang, Xia et al. 2017). These appendages have different roles in the cell. While distal appendages are required for ciliogenesis and lysosome release immunological neural connections (Tanos, Yang et al. 2013) , (Stinchcombe, Randzavola et al. 2015), whereas subdistal appendages are responsible for microtubule formation and movement of cilia in multicliated cells (Gorgidze and Vorobjev 1995) and (Kunimoto, Yamazaki et al. 2012).

Centriolar microtubules are modified by posttranslational modifications such as glutamylation, which is different then the state of cytoplasmic microtubules(Bobinnec,

Moudjou et al. 1998). Exploiting this natural distinction, Bobinnec and partners treated HeLa cells with polyglutamylation antibodies and found that deglutamylation resulted in mitotic phenotypes (Bobinnec, Khodjakov et al. 1998). Besides equal chromosome segregation role of the centrioles in spinde poles, it is also important to make sure that every cell has main base of primary cilium (Friedlander and Wahrman 1970).

Although scientists for a long time assumed that centrioles are essential for cell division, we now know that they are not. The evolutionarily conserved function of the centrioles is the formation of the primary cilium. To assemble the primary cilium, centrioles move to plasma membrane and the mother centriole functions as the basal body to nucleate the assembly of the ciliary axoneme. Mutations of proteins that play key roles in primary cilium assembly and function cause the genetic diseases termed ciliopathies(Marshall and Nonaka 2006).

2.1.2 PERICENTRIOLAR MATERIAL

Pericentriolar material (PCM) is a matrix of proteins that nucleate and organize microtubules. Centrioles recruit PCM to form the centrosome. The gamma-tubulin ring complex that localize to PCM assigns centrosomes the MTOC function. Although PCM has long been thought as a matrix of amorphous material, the recent advances in superresolution microscopy revealed a very ordered organization (Gould and Borisy 1977). Superresolution-based spatial mapping of different PCM proteins define the architecture of PCM. For example, during PCM assembly, Pericentrin (PCNT) is recruited to the centrioles wall that localizes in the PCM in an elongated manner and the rest of the proteins forms rings of different diameters (Lawo, Hasegan et al. 2012). Also, this hierarchical assembly of PCM is conserved across different species and was mapped in detail both in *Drosophila* embryos and mammalian cells (Mennella, Keszthelyi et al. 2012). Importantly, these studies also revealed the molecular basis of the dynamic nature of centrosomes during cell cycle. During mitosis, PCM enlarges with accumulation of more PCM proteins and their organization within PCM also changes. Mitotic kinases such as Polo Like Kinase 1 (PLK1) (Lane and Nigg 1996) and Aurora A (Hannak, Kirkham et al. 2001) play key roles in regulting the PCM1 dynamic assembly during mitosis (Lee and Rhee 2011).

2.1.3 CENTRIOLAR SATELLITES

Centriolar satellites are 70-100 nm, electron dense granules that localize and move around centrosomes. They are now defined as the third component of the vertebrate centrosome/cilium complex. Although satellites are ubiquitous structures in vertebrate cells, there is variation in their number, size and composition in response to differen stimuli and across different cell types and tissues. In fibroblasts and epithelial cells, they are mostly clustered around the centrosomes and to a less extent scattered evenly throughout the cytoplasm. While they concentrate around the nuclear envelope in myotubes, they are scattered below the basal bodies in the apical side of multiciliated epithelial cells. Like centrosomes, centriolar satellites are macromolecular protein complexes. Their assembly is scaffolded by PCM1 (pericentriolar material 1), which is the molecular marker for centrosomes (Dammermann and Merdes 2002), (Balczon, Bao et al. 1994) and (Kubo and Tsukita 2003). In addition to the regulation of centrosome and cilium complex, new findings show that it has serious roles such as cilium formation, centrosome duplication, autophagy and neurogenesis (Firat-Karalar, Rauniyar et al. 2014) and (Tollenaere, Mailand et al. 2015).

2.2 CILIA

Cilium is a microtubule-based structure that is extended from cell membrane. Cells need to exit from cell cycle and enter to G0/G1 phase to form a cilium. There are two main types of cilium which are motile cilia and primary cilia. Almost every cell in our body has a single, immotile primary cilium. Primary cilium functions as the cellular antenna that receives and transmits developmentally important signaling pathways such as Hedgehog signaling, Wnt signaling among others (Satir, Pedersen et al. 2010). Even though primary cilia has long been thought as nonfunctional organelles, research in the last 20 years showed that that cilia play key roles as the signalling center. Primary cilium initiates several pathways that responds to mechanical and chemical stimuli. Hedgehog signalling pathway is one of the best characterized cilium-regulated signaling pathway, the receptors of which localize to the primary cilium to sense and transmit the Hedgehog stimuli to the nucleus to initiate transcription. There are three

main structures to form a cilium, which include the basal body, axoneme and transition zone. The mother centriole converts into the basal body during cilium formation and nucleate the formation of the microtubule-based ciliary axoneme. Transition zone is a gate between basal body and axoneme, which regulates what proteins go in and out of the cilia (Marshall 2008). Three protein modules termed CEP290, NPHP and MKS comprise transtion zone, and they function with BBSome and IFT complexes to efficiently transport proteins within the cilium(Goncalves and Pelletier 2017). Cells must exit the cell cycle and enter G0 to assemble the primary cilium. Cilium assembly is initiated with Rabin8 guanine nucleotide exchange factor and Rab8 GTPase activation during G0, and they promote the localization of the ciliary vesicles (CV) to the mother centriole's distal appendages. After this process, distal end of the mother centriole is re-shaped and microtubule protraction from mother centriole forms the cilium axoneme (Sanchez and Dynlacht 2016).

Specialized epithelia in human body bear motile cilia that move liquid along cells and are key to the functions of these cells In the fallopian tube, motile cilia carry the egg to the endometrium with ciliary movement (Croxatto and Ortiz 1975); they also beat to remove the mucus from the surface of trachea epithelial cells (Ganesan, Comstock et al. 2013) and they are found in brain ventricles to bump cerebrospinal fluid (CSF) (Faubel, Westendorf et al. 2016). The ciliary axoneme of the motile cilia is significantly different from the one of the primary cilium in terms of its composition and structure. For example the cilia in brain ventricals have microtubule doublets which have 9+0 pattern (Pennekamp, Menchen et al. 2015), but sperm flagella and Fallopian tube cilia are organized with a 9+2 microtubule doublet (Raidt, Werner et al. 2015). Another type of motile cilia in human body is the flagellum of sperm cells, which is required for the motility of the whole cell. Defects in motile cilia assembly and function are implicated in genetic diseases termed primary ciliary dyskinesia (PCD), which is characterized by respiratory problems, infertility and situs inversus.

2.3 CENTROSOME BIOGENESIS

During cell cycle, centriole duplication process is initiated at the end of G1 phase and during S phase. New centriole called as "procentriole" is nucleated from the pre-

existing parental centrioles to form its basic structure. During S and G2 phases, it grows to reach a fully mature state. After centrioles are formed, PCM proteins are recruited around them. High resolution imaging experiments showed that PCM accumulation is mainly observed around mother centriole (Sonnen, Schermelleh et al. 2012). The two centrioles of the interphase centrosomes are connected by a proteinaceous linker composed of various proteins such as C-NAP1 and Rootletin (Mayor, Stierhof et al. 2000) and (Bahe, Stierhof et al. 2005). This linkers keeps the two centrioles together and ensures that there is only one major microtubule organizing center in cells. Before a cell enters mitosis, Salvador (hSav1) and mammalian sterile 20-like kinase 2 (Mst2) which are Hippo pathway proteins cause the phosphorylation of Never In Mitosis A-related kinase 2 (NEK2). Phosphorylated NEK2 plays critical role in the separation of two centrioles by phosphorylating CNAP-1 and Rootletin. Nek2-mediated phosphorylation degrades the connecting fibers between two centrioles and duplicated centriole pairs can move separately and form microtubules from two sides of the cell. Movement of the isolated centrosomes is then kept up by Eg5-microtubule pathway (Mardin, Lange et al. 2010).

An earlier report showed that the centriole loss in centrosome causes diffusion of PCM and then complete centrosome destruction in human cells (Bobinnec, Khodjakov et al. 1998). After this study, another group demonstrated that the size of the centriole is a factor which determines the amount of PCM accumulation around centrosome, and they observed greater PCM in *C.elegans* which have bigger centrioles (Kirkham, Muller-Reichert et al. 2003). On the side of the discoveries, a group found a progressive centriole-less cell formation during centriole duplication in a Drosophila strain likewise prompted the destruction of PCM in those cells (Basto, Lau et al. 2006). All examinations highligt the significance of centrioles to form a proper centrosome, so we should figure out how a centriole is assembled to explain centrosome biogenesis.

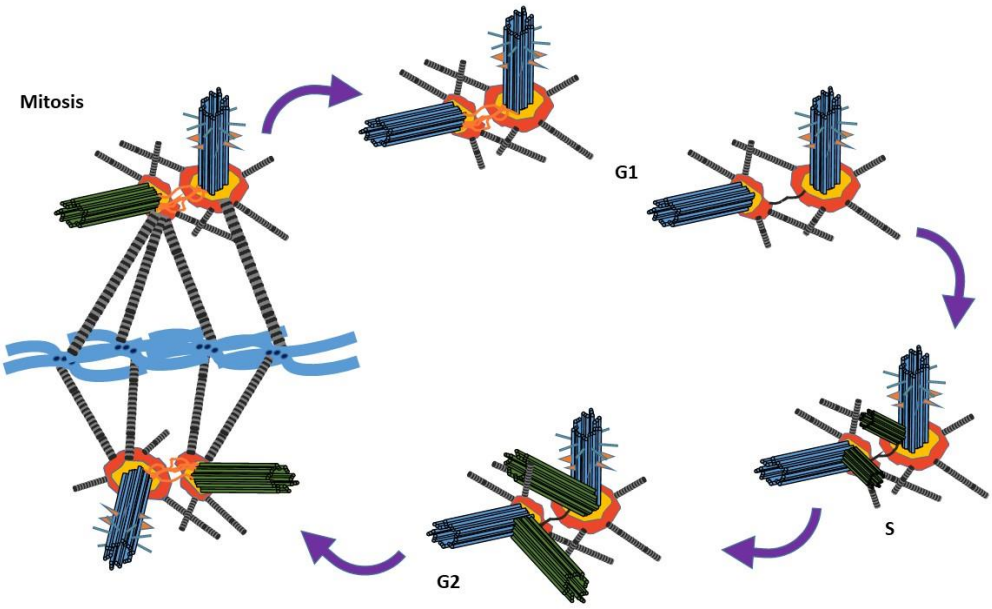

Figure 2.2 Centrosome Duplication in different phases When cells grow enough for a new cycle, fibers (orange in the figure) between centrioles break down at the G1 phase to be able to form a new centriole. Centriole splitting is followed by new centriole synthesis, and then these centrioles are matured in G2 phase. Mature centrosomes go to spindle poles to form spindle microtubules and to separate chromosomes during mitosis. (Lee and Rhee 2011).

2.3.1 CENTRIOLE ASSEMBLY

There are two major pathways that mediate centriole duplication. First one is *de novo* centriole assembly and the second is the canonical duplication of centrioles. Canonical centriole duplication is the one where the pre-existing parental centrioles function as the template to nucleate the assembly of new centrioles. *De novo* centriole duplication is the one that takes place without a pre-existing centrioles, which has recently been nicely demonstrated in multiciliated epithelia (Anderson and Brenner 1971).

The master regulator for canonical centriole duplication is PLK4, which initiates the duplication process during S phase. When PLK4 is recruited to the pre-existing centrioles, it initiates the duplication pathway to assemble procentrioles. PLK4 centriolar recruitment is regulated by various proteins such as CEP63, CEP152 and CEP192. CEP63 and CEP152 proteins have the centrosomal ring localizations with different width (Brown, Marjanovic et al. 2013) and (Lukinavicius, Lavogina et al. 2013) and they form the scaffold for PLK4 recruitment. PLK4 first forms the ring structure

then it changes its localization as a single spot at the proximal end. SAS-6 protein which is used to label newly formed centriole at later phases of the duplication process also localizes in the same place with PLK4 dot (Kim, Park et al. 2013).

After PLK4 recruitment, another centriole duplication protein STIL is recruited to the centriole and these two proteins together mark the site of centriole duplication. Once recruited, STIL further activates and stabilizes PLK4. Following PLK4 and STIL recruitment, SAS-6 is recruited to the site of centriole duplication. SAS-6 functions as the template for the nine fold symmetric centrosome structure. The oligomer of SAS-6 that functions as the template is known as cartwheel (Keller, Orpinell et al. 2014). A study adduced that this cartwheel was thefundamental structure to form the nine fold symmetric centriole because centrioles of *Chlamydomonas* which have mutated bld12, Sas-6 homologue, are formed with folds that differed from nine(Nakazawa, Hiraki et al. 2007). On the other hand, a recent study showed that artificially produced Sas-6 proteins which can from carthwheel with different symmetries can still generate nine fold symmetric bases. This indicates that Sas-6 works with different components for the centriole structure (Hilbert, Noga et al. 2016). Despite the fact that Sas-6 affects centriole biogenesis in different ways, it is obvious that this protein has a critical role in both centriole and basal body formation (Leidel, Delattre et al. 2005) and (Hu, Liu et al. 2015).

CPAP protein works with CEP120 and SPICE1, and they start to prolong the microtubules in the centrioles after cartwheel is formed (Comartin, Gupta et al. 2013). New studies about CPAP and centriole growth help to explain the role of CPAP in this process. A group demonstrated that the PN2.3 region of the protein physically interacts with an exposed beta tubulin site at the plus ends of the microtubules to promote slow and controlled centriolar microtubule growth (Sharma, Aher et al. 2016). After this study, another group showed that the mutations on the 375th and 343rd aminoacids in the region of CPAP cause centriole biogenesis abnormalities which are shorter or longer depending on the mutated amino acid (Zheng, Ramani et al. 2016). As well as the mutation, overexpression of CPAP also results in prolonged centrioles and as a natural structure these centrioles are capped by CP110 from their distal ends. Strikingly, combination of CPAP overexpression and CP110 reduction

causes huge centrioles which have 8 micrometer in length (Schmidt, Kleylein-Sohn et al. 2009). Since over- and low- expression levels of CP110 affects on centrosome and cilium biogenesis oppositely, the amount of CP110 is considered as a strong determinant of centriol length (Spektor, Tsang et al. 2007).

Second way of centriole formation has been called as *de novo* or "acentriolar" duplication, and it has been investigated in rhesus monkey oviducts by using an electron microscope. They found that most of the centrioles are formed with *de novo* (about 95%) while small portion of centrioles uses the old centriole as a template to replicate itself (Anderson and Brenner 1971).

Centrioles in a centrosome are duplicated to generate two centrosomes to help chromosome segregation in dividing cells (Tsou and Stearns 2006). Centriole number should be tightly regulated because abnormal chromosome segregation is one of the major reasons for cancers. It is known that most of the cancer types have abnormal centriole number (Nigg 2002). On the other hand, certain types of cells must have huge number of the centrioles to be able to form multiple cilium, so these cells use *de novo* duplication mechanism to increase their centriole number (Lemullois, Boisvieux-Ulrich et al. 1988). DEUP1 protein which is CEP63 paralogue and called as CCDC67 is the major player of *de novo* centriole duplication process. I found that DEUP1 does not work alone during *de novo* duplication, it recruits the other important components which are CEP152, PLK4 and SAS-6 to form deuterosome complexes. Since almost the same proteins are required for the duplication process which uses the older centriole as a template and *de novo* duplication, it can be the evidence showing that CEP63 may be diverg to be able to carry out massive centriole duplication, and these two duplication pathways share a common origin (Zhao, Zhu et al. 2013).

2.3.2 PERICENTRIOLAR MATERIAL ASSEMBLY

Assembly of pericentriolar material is also regulated with certain proteins. For example, overexpression of both Pericentrin (PCNT) and CDK5RAP2 causes a big sized PCM, but other PCM proteins cannot induce such overgrowth PCM, so it shows that there are different stages of PCM assembly, and PCNT and CDK5RAP2 proteins take place in the early stages. Also, high resolution microscopy images show that while C-

terminus of the PCNT protein is responsible for centrosome localization, N-terminus of the protein creates an rea for the other PCM proteins such as TUBG1, CEP152 and NEDD1 (Lawo, Hasegan et al. 2012). When centrioles mature during centriole duplication cycle, PCM assembly is also initiated that continues to grow during mitosis (Palazzo, Vogel et al. 2000). There are different mechnismis regulating PCM assembly. For example PCNT in human cells and Cnn in *Drosophila* cells need to be phosphorylated by Polo Like Kinase 1 (PLK1) to recruit more proteins to the PCM (Lee and Rhee 2011) and (Conduit, Feng et al. 2014). When PCM grows enough for cell division, centrosomes boost their microtubule nucleation capacity (Piehl, Tulu et al. 2004).

2.4 CENTROSOME FUNCTION AND DISEASE

Centrosomes function as the major microtubule organizing centers to regulate a wide range of cellular processes such as cell division, motility and cellular signaling. Accordingly, their deregulation has been associated with various human diseases including cancer, neuronal and developmental disorders (Doxsey 2001).

Nigg E. et al. previously found that cancer cells have extra centrosomes, but they were uncertain whether it is the reason for or result of the cancer cell formation because it is known that any problem in well characterized tumor-supressor gene, p53, also causes centrosome number abnormalities (Nigg et. al, 2002). Different groups have contradictory hypotheses. One of them indicates that no tumor formation is observed in the mouse with overduplicated centrosomes but lots of mitotic problem were observed in the cultured cells of the same mouse (Vitre, Holland et al. 2015). However two recent studies show that centrosome number abnormalities cause tumor formation in mice through different proteins which are PLK4 and NLP & CEP131 respectively (Levine, Bakker et al. 2017) and (Ganier et al. 2018).

Mechanisms behind centrosome number dependent cancer formation are more obvious. Because Boveri et al. observed multipolarity in dispermic sea urchin egg cells because of the centrosome number abnormalities, they think that this kind of mitotic defects may be the reason for missegregated chromosomes and then boosted tumorigenesis (Boveri 2008). Recent studies have shown that cancer cells which have

overduplicated centrosomes form bipolar spindles by collecting their centrosomes into the opposite sites of the cells. Because the cells which have multipolar spindles are unhealthy and unstable, cancer cells develop a compensatory mechanism (Brinkley 2001). This kind of gathering of extra centrosomes into two spindle poles is known as "centrosome clustering", and motor proteins, microtubules and actin cytoskeleton are three key elements for the process (Kwon, Godinho et al. 2008). Until centrosomes are clustred, spindle microtubules coming from every single centrosome bind to chromosomes and because of the movement of the centrosomes, and dynamicity of the microtubules, extra centrosomes can cause instability in the rate of oncogenes and tumor supressors (Beroukhim, Mermel et al. 2010) and (Ganem, Godinho et al. 2009).

Most of the studies suggest that centrosome is not essential to form bipolar spindle poles. A study in which centrosomes were depleted by using laser microsurgery showed that when cells lose their centrosome they have compensatory mechanisms to complete bipolar cell division (Khodjakov, Cole et al. 2000). Also, we know that plant cells do not have any centrosome, but they can still divide properly, so it is obvious that centrosome is not required for cell division (Szollosi, Calarco et al. 1972) and (Lloyd 1989).

Centrosome has several functions such as cell migration and polarity during interphase, so centrosome number abnormalities also disrupt these functions thereby tissue structure (Kushner, Ferro et al. 2014). Centrosome depletion in migrating cells also changes directionality and decreases the migration velocity (Wakida, Botvinick et al. 2010).

The most important fuction of the centrosome is to form both motile or nonmotile cilia during G0 phase by using mother centriole as a template (Conduit, Wainman et al. 2015). Two types of cilia have different functions. For example primary cilium which is a nonmotile cilium is known as a cellular antenna, and it is responsible for receiving and transmitting signals for several pathways such as Sonic Hedgehog and (Singla and Reiter 2006) since these pathways have a role during developmental stage, defects on primary cilium affect cellular differentiation (Falcon-Urrutia, Carrasco et al. 2015) and (Fu, Asp et al. 2014).

Roles of motile cilia are different from the primary cilium. Multi-ciliated cells are required for creating movement outside of the cell to remove mucus from trachea and they form left-right symmetry over nodular flow (Kunimoto, Yamazaki et al. 2012) and (Nonaka, Tanaka et al. 1998). Also, sperm cells in mammals and many unicellular organisms with centrosome have flagella which are another type of motile cilia with longer microtubules flagella are used to gain motility (Mitchell 2007).

Most of the vertebrate cells have one or more cilia in terms of their functions (Rieder, Faruki et al. 2001) and defective cilia can be causative agent for diseases named “ciliopathies” (Zariwala, Knowles et al. 2007). If cells do not form cilia or they do not have centrosome/cilium complex, they will not complete their differentiation and they cause problems during early developmental stages (Bazzi and Anderson 2014).

Thus, if there is a mutation on the genes which encode cilium related proteins, it may affect whole body parts such as kidney, brain and trachea (Waters and Beales 2011).

2.4.1 Microcephaly

Defective cilia in the brain cause a severe disease which is autosomal-recessive primary microcephaly (MCPH) and these patients have developmentally problematic smaller brain cortex. There are twelve identified mutations causing primary microcephaly. Interestingly, ten mutations were identified in the genes whose products localize at centrosome or are important for spindle pole localization (Hussain, Baig et al. 2012). The other two genes are CASC5 and ZNF335 which are kinetochore and nucleus related, respectively (Cheeseman, Hori et al. 2008) and (Yang, Baltus et al. 2012). Indeed, centrosome has been shown to play a role in various cellular processes affecting brain development and depletion of the neural progenitors develop microcephaly in the brain of mouse with extra centrosome (Kuijpers and Hoogenraad 2011) and (Marthiens, Rujano et al. 2013). Strikingly, Zika virus infection causes microcephaly related phenotype, so a study show that 3-D culture of infected brain cells develop microcephaly and these cells have similar problems like structural defect on centrosome (Gabriel, Ramani et al. 2017).

2.4.2 Retinal Degeneration

Retinal photoreceptor neurons are profoundly differentiated to respond photons. They have a separated structure divided into inner and outer segments. These two segments have different functions. While inner segment produces energy and expresses protein, outer one, with its cone and rod shape, senses the photons (Brockerhoff and Fadool 2011). Elongated cilium forms the outer section of these receptors and motor proteins working together with intraflagellar transport protein 88 (IFT88) to control their formation (Marszalek, Liu et al. 2000) and (Pazour, Baker et al. 2002).

One of the most common ciliopathies is retinal degeneration and it is because of the defects on photoreceptors. Various studies show that this disease is commonly result of the mutations of certain centrosome and cilium proteins (Hong, Pawlyk et al. 2003), (Liu, Zhou et al. 2002) and (Conkar, Culfa et al. 2017).

2.5 EVOLUTION OF THE CENTROSOME

Centrosome is assigned as a name for a central organelle in the cell, and it is known that it can protect its localization which is at the center of the cell and near the nucleus during interphase and duplicate itself for mitosis. Also, centrosome is the major player in the cell to form and to regulate microtubules. Distinct shapes of the centrosome were identified for different eukaryotic cells but most of them contain centrioles (Kilmartin 2003) and (Mana-Capelli, Graf et al. 2009).

Eukaryotes share a conserved structure which is flagellar apparatus, but its structure for different species is well investigated and their conservation patterns are identified. Eukaryotes form their flagellates by using flagella's basal bodies as a template, so it may be the evidence to show that they are coming from the same origin (Leadbeater B.S.C et al. 2000). Different analysis show that animals and Amoebozoa might not share the same ancestor for their centrosome structure, and it is very well known that eukaryotic centrosomes have a common structure (Azimzadeh 2014).

2.6 CELL DIVISION

Almost all cells generate new progenies when they reach the enough size and the necessary conditions are met. During cell division, cells increases the number of organelles and most of the proteins, but they just duplicate their DNA and centrosome only once in every cell cycle.

2.6.1 Eukaryotic Cell Division

There are two types of cell division for eukaryotic cells, and these are mitosis and meiosis. While meiosis event is observed only in germ cells, mitosis is more frequent for eukaryotes. For every cycle, cells have two major phases which are interphase and mitosis. These two phases have sub-stages. G1, S and G2 are the sub-stages of the interphase (Norbury and Nurse, 1992). G1 phase is necessary for cell growth and preparation of DNA duplication. During G1 phase, cell may decide to exit from cell cycle if environment is not good enough for division, and cell enters G0 phase. If cell continuous to cell cycle, S phase will follow G1 phase. During synthesis phase, cell copies its DNA and centrosome, and it completes these processes during G2 phase. After DNA and centrosome duplication, cell prepares its every component to divide in G2. Mitosis is one of the main pahses to segregate chromosomes equally to the new progenies. There are also four sub-pahses of mitosis which are prophase, metaphase, anaphase and telophase. In the beginning of the anaphase main cell starts separation to form two identical cells, and this process is called as cytokinesis (Sivakumar and Gorbsky, 2015).

2.6.2 Regulation of Cell Division

Three important checkpoints and expression levels of the cyclin proteins regulate the division process. G1/S, G2/M and spindle assembly chekpoints are the regulation points of the cell cycle (Harashima and Dissmeyer, 2013). Cells control the process through the checkpoints which are important to be sure that the environment is suitable for division and they have two copies of DNA and each chromosome pairs are holded by spindle microtubules, respectively. Cells also check the DNA integrity and sequence to prevent mutations after DNA synthesis. When a mutation is detected on

DNA, cell does not continue to cell cycle to fix the mutation. Also, if there is an alignment problem for the sister chromatids during metaphase, cell cycle will be arrested in the third checkpoint. (Vermeulen and Van Bockstaele, 2003). There are various type of DNA damage such as single strand break (SSB) and double stranded break (DSB), and ATR and ATM kinases are the responsible proteins to detect these during DNA syntesis, respectively. Chk1 and ChK2 are kinases which are the first activated proteins to control mutations in G1 and G2. The last checkpoint, SAC, is activated to be sure that all chromosomes are attached by spindle microtubules from both sides, properly to avoid aneuploidy (Saurin et al., 2011). Another important protein family is Cyclin-dependent kinases (Cdks), which show cyclin dependent activity and regulates the division process. Eventhough expression levels of the CDKs' regulatory proteins, cyclins, change according to cell cycle stages, CDK expression levels are the same during mitosis (Hopkins and Tyson, 2017). To exit mitosis, cells need to regulate the degradation process of the mitotic proteins, so there is a ubiquitin ligase protein which is called as "anaphase promoting complex/cyclosome (APC/C)". This protein ubiquitinylates its targets cyclin A and cyclin B to direct the cell to the cytokinesis (Eggert and Field, 2006) and (Peters, 2006).

3 CCDC57

Centrosomes function as main microtubule-organizing centers of animal cells and mediate various key cellular and developmental processes including cell shape, polarity and motility, as well as spindle formation and chromosome segregation (Paz and Luders, 2018; Wu and Akhmanova, 2017). At the core of centrosomes are two centrioles, which are barrel-shaped, microtubule-based structures characterized by evolutionarily conserved radial nine-fold symmetry (Azimzadeh and Marshall, 2010; Gonczy, 2012; Winey and O'Toole, 2014). Centrioles form the centrosome by recruiting pericentriolar material (PCM), which nucleates and organizes microtubules. Additionally, centrioles nucleate the formation of the cilia and flagella, microtubule-based cellular extensions with key functions in cellular signaling and cell motility (Heydeck et al., 2018; Mirvis et al., 2018). In addition to centrioles and PCM, vertebrate cells have an array of membrane-less 70-100 nm granules that localize and move around the centrosomes in a microtubule and molecular motor-dependent manner, termed “centriolar satellites” (Hori and Toda, 2017; Kubo and Tsukita, 2003).

Deregulation of the biogenesis and functions of centrosomes and cilia are associated with various human diseases (Bettencourt-Dias et al., 2011; Nigg and Raff, 2009). Structural and numerical centrosome abnormalities were among the first cell biological defects reported in cancer (Nigg and Holland, 2018). Centrosome amplification promotes aneuploidy and invasive behavior in cultured cells (Ganem et al., 2009; Godinho et al., 2014; Kushner et al., 2014; Silkworth et al., 2009) and development of spontaneous tumors in multiple tissues in mouse models (Levine et al., 2017; Sercin et al., 2016). The sufficiency of centrosome amplification in initiating tumorigenesis was further supported by its detection before transformation in Barrett’s esophagus, which was repressed by p53 (Lopes et al., 2018). Structural centrosome abnormalities, namely the enlargement of the PCM, was shown to contribute to cancer cell invasion by a non-cell-autonomous mechanism leading to cell budding (Ganier et al., 2018a; Ganier et al., 2018b).

Mutations affecting centrosome components also cause various human developmental disorders including the autosomal primary recessive microcephaly

(MCPH) and ciliopathies. MCPH is a neurodevelopmental disorder characterized by small brain size and mental retardation, which is caused by reduced neuronal proliferation during embryonic development. Importantly, majority of the genes mutated in MCPH encode centrosome proteins with functions ranging from centriole duplication to spindle pole organization (Jayaraman et al., 2018; O'Neill et al., 2018). Eight of these proteins including PLK4, STIL, Cep63 and Cep152 function in centriole duplication, suggesting a strong link between neurogenesis and centriole number control (Nigg and Holland, 2018). Additionally, defects in centriole assembly and function impacts cilia biogenesis and function and cause ciliopathies, which are characterized multiple symptoms including renal disease, retinal degeneration, polydactyly, neurocognitive deficits and obesity (Braun and Hildebrandt, 2017; Reiter and Leroux, 2017). To determine how centrosomal defects contribute to these diseases, it is essential to elucidate the control mechanisms that regulate centrosome biogenesis and function.

Centrioles duplicate exactly only once in most cell types and this canonical duplication cycle is tightly regulated in a cell-cycle linked manner (Nigg and Holland, 2018). Centriole duplication begins with the assembly of a procentriole orthogonal to the proximal end of each pre-existing centriole during G1/S transition. Procentrioles elongate throughout S and G2 phases and are then segregated to the daughter cells by the mitotic spindle in mitosis. The mechanisms the determines the location of centriole duplication on the preexisting centrioles (hereafter the origin of centriole duplication) and dictates the orientation and copy number of procentrioles have long been areas of extensive investigation (Firat-Karalar and Stearns, 2014). Genomics, proteomics and bioinformatics studies and genetic screens identified five conserved components required for initiation of centriole duplication, which are PLK4, Cep192, SAS-6, STIL and CPAP in mammalian cells (Dammermann et al., 2004; Delattre et al., 2004; Kirkham et al., 2003; Leidel et al., 2005; Leidel and Gonczy, 2003; O'Connell et al., 2001; Pelletier et al., 2004a). Centriole duplication initiates with the recruitment of the Polo-like kinase family member PLK4 to origin of centriole duplication (Bettencourt-Dias et al., 2005; Habedanck et al., 2005). Subsequently, PLK4 phosphorylates STIL and enables it to recruit SAS-6, which oligomerizes and promotes

the formation of the nine-fold symmetrical scaffold of the centrioles termed the "cartwheel" (Arquint et al., 2015; Dzhindzhev et al., 2017; Kitagawa et al., 2011; McLamarrah et al., 2018; Nakazawa et al., 2007; van Breugel et al., 2011). Cep135 and CPAP then binds to the SAS-6/STIL scaffold and initiates the assembly and stabilization of microtubules around the cartwheel (Arquint and Nigg, 2016; Lin et al., 2013a; Ohta et al., 2002).

Timely and efficient recruitment of PLK4 to the origin of centriole duplication is a key step during centriole duplication that is regulated at multiple levels. First, the cellular abundance and kinase activity of PLK4 is regulated through phosphorylation and ubiquitination (Cunha-Ferreira et al., 2013; Guderian et al., 2010; Holland et al., 2012; Klebba et al., 2013). Second, its centrosomal targeting requires the cooperative action of multiple protein scaffolds at the proximal end of centrioles in mammalian cells. Cep152 and Cep192 are the components of the first scaffold, which recruit PLK4 to the centrioles through the electrostatic interactions with its negatively charged polo-box domain of PLK4 (Cizmecioglu et al., 2010; Hatch et al., 2010; Kim et al., 2013; Sonnen et al., 2013). The centrosomal recruitment of Cep152 is in turn regulated by Cep63, which is not a conserved core duplication protein but functions in ensuring efficient centriole duplication (Brown et al., 2013; Sir et al., 2011). Recent in vitro studies identified the self-assembly of Cep63 and Cep152 into higher-order cylindrical architectures as the underlying mechanism for PLK4 recruitment (Kim et al., 2019).

In addition to conserved components of the centriole duplication pathway, some proteins are unique to vertebrates, where centrosomes have more complex roles during development and differentiation. An example to this diversity is in the composition of the protein scaffolds that recruit PLK4 to the origin of centriole duplication. While PLK4 recruitment depends on Asterless in flies and Spd-2 in nematodes, the homologues of these two distinct proteins, Cep152 and Cep192, cooperate during this process in mammalian cells (Dzhindzhev et al., 2010; Kemp et al., 2004; Kim et al., 2013; Pelletier et al., 2004b; Sonnen et al., 2013). Another example is the regulation of centriole duplication by centriolar satellites, which are vertebrate-specific membrane-less granules that localize and move around the centrosomes in a microtubule and motor-dependent manner (Hori and Toda, 2017; Kubo et al., 1999).

The centriolar satellite proteins CCDC14, KIAA0753, SPAG5, Cep72 and Cep90 were shown to function in centriole duplication by regulating centrosomal targeting of duplication proteins, in particular the ones mutated in primary microcephaly such as Cep63 (Firat-Karalar et al., 2014; Kodani et al., 2015).

To identify new regulators of centrosome biogenesis in mammalian cells, we previously generated proximity interaction maps for proteins that function during initiation of centriolar duplication including Cep63 and its paralog Deup1, PLK4, Cep152, CPAP and Cep192 using the proximity-dependent biotin identification (BioID) approach (Firat-Karalar et al., 2014). CCDC57 was one of the uncharacterized proteins that stood out in these maps due to its high proximity to centriole duplication proteins. Notably, CCDC57 was recently identified as a component of the centriolar satellite interactome, which corroborates the functional relationship between centriolar satellites and centriole duplication (Gheiratmand et al., 2019). Here, we characterized CCDC57 as a new centriole duplication protein required for recruitment of the microcephaly-associated proteins Cep63 and Cep152 to the centrosome. Moreover, independent of its centrosomal targeting, CCDC57 localizes and binds to microtubules and regulates microtubule nucleation, stability and mitotic events like chromosome alignment and cytokinesis. Together, our results identify CCDC57 as dual regulator of centriole duplication and mitotic progression and provides insight into disease mechanisms that underlie primary microcephaly.

3.1 Results

3.1.1 CCDC57 localizes to the centrosome and centriolar satellites

We previously identified CCDC57 as a proximity interactor for centriole duplication proteins (Firat-Karalar et al., 2014). Another BioID-based screen recently also revealed proximity interactions of CCDC57 with centriolar satellite proteins and confirmed partial co-localization of Flag-CCDC57 at the centriolar satellites in HEK cells (Gheiratmand et al., 2019). To test whether, and if so, where endogenous CCDC57 localizes at the mammalian centrosome/cilium complex, we examined its endogenous localization in human osteosarcoma U2OS cells using a CCDC57 polyclonal antibody that recognizes the 508-620 amino acid fragment of human CCDC57 (Figure 3.1A). CCDC57 localized to the centrosome throughout the cell cycle, as assessed by co-localization with the centriole marker centrin (Figure 3.1B). While a similar localization pattern to the centrosome was observed for transiently expressed myc-CCDC57, ectopic fusion protein also localized to a subset of centriolar satellites, as assessed by co-localization with the centriolar satellite marker PCM1 (Figure 3.1C). The satellite pool of CCDC57 identified when it is expressed ectopically confirms its affinity to the centriolar satellites but does not reveal satellites. Together, these results identified CCDC57 as a bona fide centrosome protein.

Spatial localization of proteins at the centrosome informs hypothesis about their function. To determine the high-resolution localization of CCDC57 at the centrosome and basal body, we performed super resolution OMX microscopy for U2OS cells stained for CCDC57 along with markers of the distal lumen proteins (Centrin 3), proximal end linker proteins (C-Nap1, Rootletin), PCM proteins (Cep63 and Gamma-Tubulin) and appendage protein (CEP164). CCDC57 localization at the centrosome was proximal to that of centrin and CEP164 and distal to that of C-Nap1 and Rootletin (Figure 3.2). Like Cep63, CCDC57 localized to resolvable rings at the proximal end of centrioles. However, the proximal rings of Cep63 and CCDC57 only partially co-localized (Figure 3.2). These results map CCDC57 to the proximal end of the centriole.

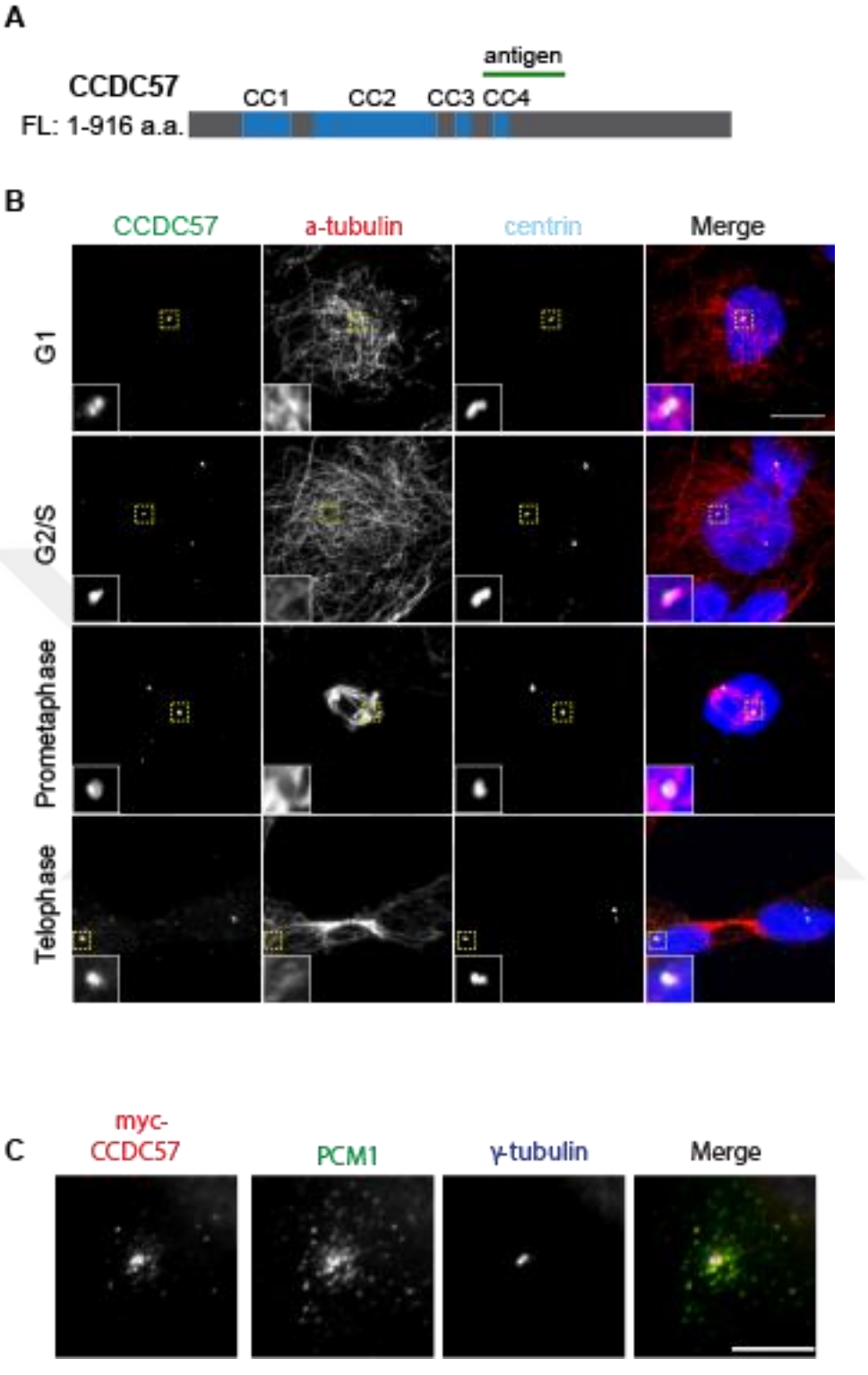
A
antigen
CCDC57
CC1
CC2
CC3
CC4
FL: 1-916 a.a.
B
CCDC57
a-tubulin
centrin
Merge
G1
G2/S
Prometaphase
Telophase
C
myc-CCDC57
PCM1
γ-tubulin
Merge

Figure 3.1 CCDC57 is a centrosomal protein. (A) Schematic of CCDC57 full length (FL) construct. Numbers indicate CCDC57 amino acids. CC indicate coiled coil domains. The antibody used in this study was raised against the 508-620 amino acid fragment of human CCDC57. (B) Localization of endogenous CCDC57 at the indicated cell cycle stages. Asynchronously growing U2OS cells were fixed and stained for CCDC57, alpha-tubulin and centrin 3. (C) myc-CCDC57 localizes to the centrosome and centriolar satellites. U2OS cells transfected with myc-CCDC57 were fixed and stained for myc, PCM1 and γ-tubulin. DNA was stained with DAPI. Scale bars, 10 µm, all insets show 4x enlarged centrosomes

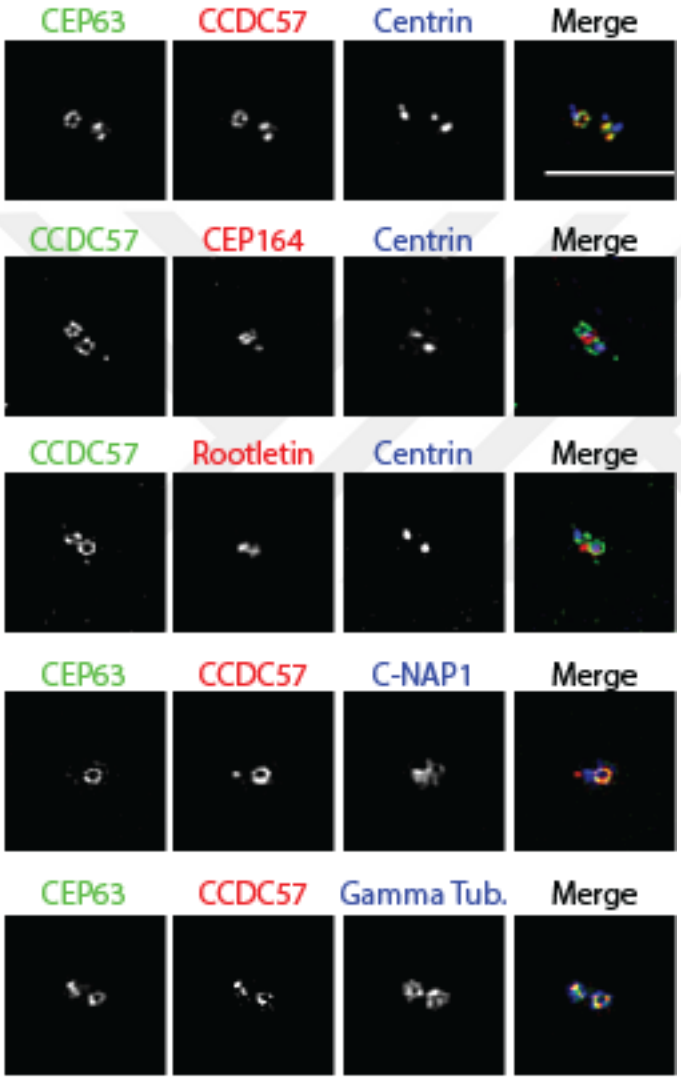

Figure 3.2 CCDC57 localizes to the proximal end of the centriole. Representative super resolution OMX micrographs were shown for CCDC57 staining relative to different centrosome markers. U2OS cells were fixed and stained for CCDC57 and markers of the centriole distal lumen (Centrin 3), the pericentriolar material (Cep63 and Gamma Tubulin), appendage protein marker (CEP164) and the centriole proximal end (Rootletin, C-Nap1). Scale bar, 3 μm.

3.1.2 CCDC57 localizes to centrosomes and microtubules through distinct regions

CCDC57 has four coiled coil domains at its N-terminal 1-605 amino acid region (CC1: 92-173, CC2:214-422, CC3:456-483, CC4:521-548) and no identifiable domains at its C-terminal 606-916 amino acid region (Figure 3.3A). To determine the regions required for its localization to centrosomes, we generated a series of GFP-fusion deletion constructs and ectopically expressed them in U2OS cells for localization experiments (Figure 3.3A). The GFP-CCDC57 (1-502) and (1-605) fragments localized to the centrosome during interphase and mitosis (Figure 3.3B, 3.4A). Their co-localization with two centrin foci in interphase and four centrin foci in mitosis confirm their localization at the centrosome and identify the first 502 amino acids as the centrosomal targeting domain (Figure 3.3A).

The C-terminal GFP-CCDC57 (502-916) and (606-916) fragments localized only to the microtubules, but not to the centrosome (Figure 3.3B, 3.4B). In mitotic cells, GFP-CCDC57 (503-916) and (606-916) localized to spindle microtubules during metaphase (Figure 3.3B, 3.4A). The localization experiments show that CCDC57 is targeted to centrosomes and microtubules through distinct domains at its N- and C-terminus respectively.

In contrast to its C-terminal region, full-length GFP-CCDC57 did not localize to microtubules (Figure 3.3B), suggesting that the interaction between its C-terminal domain and microtubules might be inhibited by the N-terminal domain.

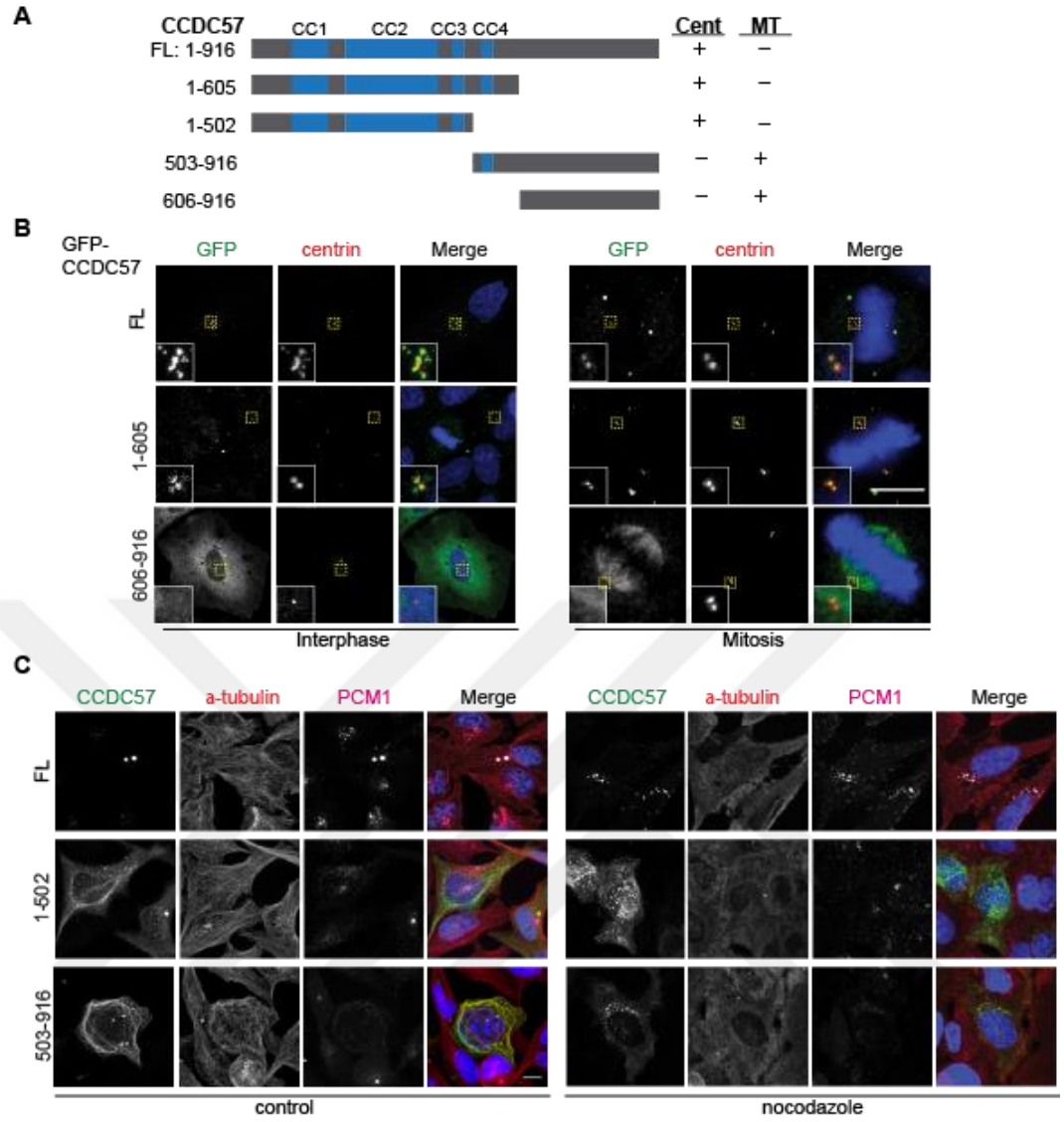

Figure 3.3 CCDC57 localizes to the centrosome and microtubules through distinct domains (A) Schematic representation of CCDC57 full length (FL) and deletion constructs and summary of their localization to the centrosome and microtubules. (B) CCDC57 (1-605) localizes to the centrosome and CCDC57 (606-916) localizes to the microtubules. Co-localization was determined by analyzing U2OS cells transfected with GFP-CCDC57 constructs and staining fixed cells for GFP and centrin. DNA was stained with DAPI. (C) Overexpression of CCDC57 and its deletion mutants disrupts centriolar satellite distribution and microtubule network organization. U2OS cells were transfected with the indicated GFP-CCDC57 constructs, treated with DMSO or 10 µg/ml nocodazole for 1 h, fixed and stained for GFP, alpha-tubulin and PCM1. DNA was stained with DAPI. Scale bars, 10 µm, all insets show 4x enlarged centrosomes.

3.1.3 Overexpression of CCDC57 and its deletion mutants disrupts centriolar satellite distribution and microtubule network organization

The pericentrosomal distribution of centriolar satellites depends on an intact microtubule network. We determined the effects of CCDC57 overexpression on the microtubule network and centriolar satellites. In high expressing cells, GFP-CCDC57 formed aggregates that sequestered endogenous PCM1 and resulted in loss of pericentrosomally distributed centriolar satellites (Figure 3.3C). In contrast, it did not change the organization of the microtubule network (Figure 3.3C). The size of the aggregates varied between different cells, which likely correlated with the relative expression level of GFP-CCDC57 (Figure 3.4C). Interestingly, PCM1 was enriched at the periphery of the aggregates, while GFP-CCDC57 was distributed homogenously. These aggregates also stained positive for centrin and Cep290, but not for other centrosome and satellite proteins including Cep63, suggesting that there is specificity in which proteins are sequestered to the aggregates (Figure 3.4D).

Overexpression of the GFP fusions of CCDC57 (1-502) and CCDC57 (503-916) resulted in formation of filamentous and granular aggregates in cells. GFP-CCDC57 (503-916)-induced bundles, but not GFP-CCDC57 (1-502)-induced ones, co-localized with microtubules (Figure 3.3C). Microtubule depolymerization upon nocodazole treatment disrupted the GFP-CCDC57(503-916)-positive microtubule bundles, indicating that it they are microtubule-based structures and expression of this fragment does not stabilize them (Figure 3.3C). In contrast, GFP-CCDC57 (1-502)-positive bundles and aggregates remained intact in nocodazole-treated cells (Figure 3.3C). Because this fragment comprises three coiled-coil domains, it is likely that these bundles resulted from dimerization of this fragment with itself or the full-length CCDC57. Finally, although GFP-CCDC57 (502-916) overexpression disrupted the distribution of centriolar satellites by clustering them around the bundles, GFP-CCDC57 (1-605) did not, suggesting that the former phenotype is likely due to a consequence of changes in microtubule organization.

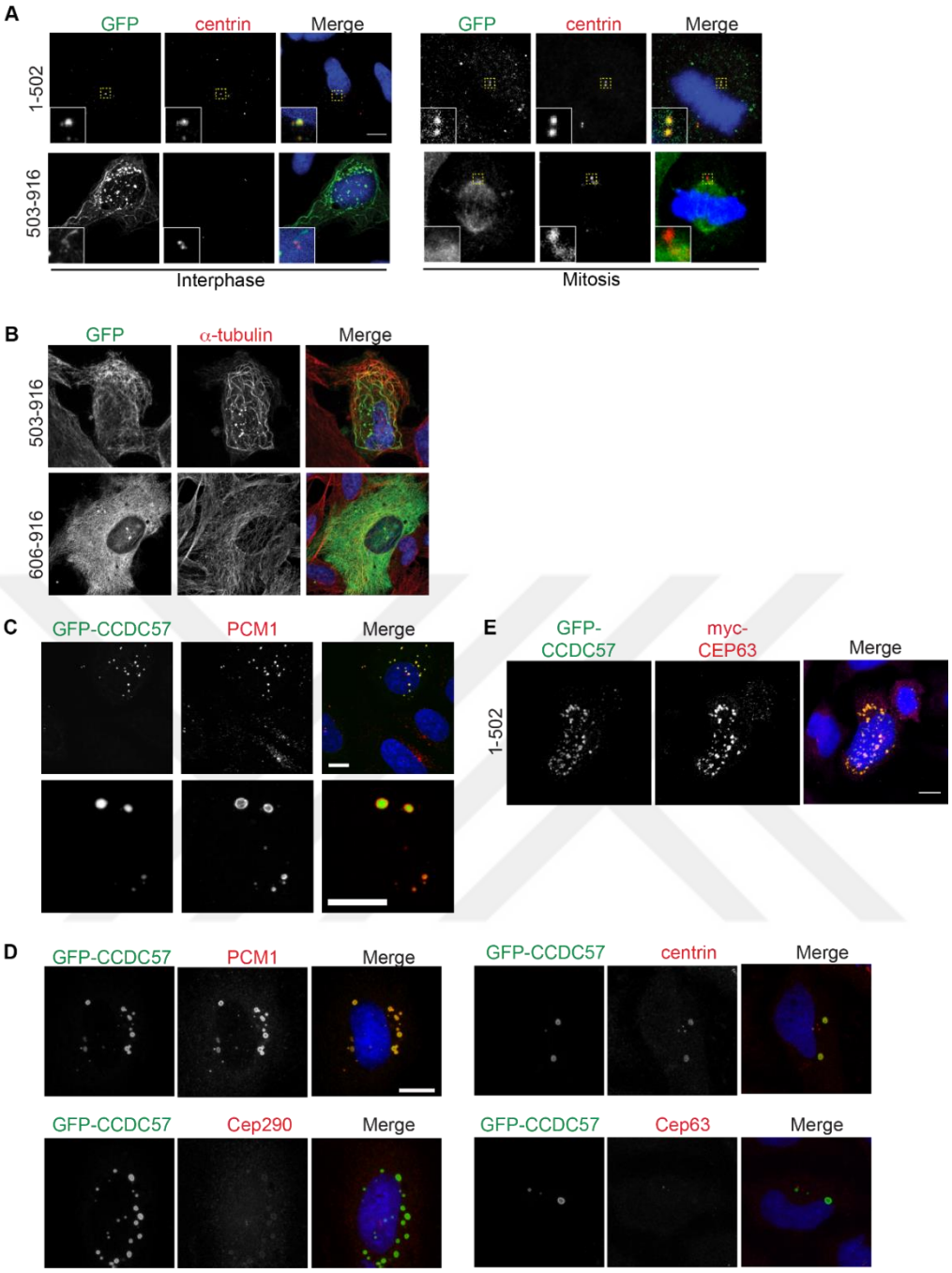
A
GFP
centrin
Merge
1-502
503-916
Interphase
Mitosis
B
α-tubulin
606-916
C
GFP-CCDC57
PCM1
D
Cep290
Cep63
E
myc-CEP63

Figure 3.4 Analysis of CCDC57 and its deletion mutants for cellular localization and overexpression phenotypes Localization of full-length CCDC57 and its deletion constructs. U2OS cells transfected with indicated constructs were fixed and stained for (A) GFP and centrin, (B) GFP and centrin or (C) GFP and alpha-tubulin. DNA was stained with DAPI. Scale bars, 10 µm, all insets show 4x enlarged centrosomes. (E) Overexpression of full-length CCDC57 disrupts centriolar satellite distribution. U2OS cells were transfected with GFP-CCDC57, fixed and stained for GFP and PCM1. (E) Overexpression of full-length CCDC57 drives localization of a subset of centrosome proteins to aggregates. U2OS cells were transfected with GFP-CCDC57, fixed and stained for GFP and antibodies against indicated proteins.DNA was stained with DAPI. Scale bars, 10 µm, all insets show 4x enlarged centrosomes.

3.1.4 CCDC57 has extensive proximity interactions with components of the centrosome/cilium complex

CCDC57 was previously identified as a proximity interactor Deup1, which functions in deutorosome-mediated centriole duplication in multiciliated tracheal epithelial cells and OFD1, which functions in cilium assembly (Gupta et al., 2015; Zhao et al., 2013). To gain unbiased insight into cellular functions and mechanisms of CCDC57, we identified the spatial proximity interactome of full-length CCDC57 and its microtubule-targeting 606-916 amino acid region using the BioID approach. N-terminal myc-BirA* fusion of CCDC57 (BioID-CCDC57) localized to and stimulated biotinylation at the centrosome and centriolar satellites, as assessed by myc and streptavidin staining (Figure 3.5A, 3.6A). BioID-CCDC57 (606-916) localized to the microtubules and stimulated biotinylation both at the microtubules and the centrosome, suggesting that it either transiently localizes to the centrosome or its interacting partners at the microtubules exchange with the centrosome (Figure 3.6A). Cells expressing the BioID fusions were incubated with 50 µM biotin for 18 h. Untransfected cells and cell expressing myc-BirA* were processed in parallel as controls. After lysis with denaturing buffer, biotinylated proteins including the baits were precipitated by streptavidin beads, as assessed by immunoblotting for myc and streptavidin (Figure 3.4B). Following mass spectrometry analysis, the proximity interactors of CCDC57 were ranked based on their normalized spectral abundance factor (NSAF) values. Gene ontology (GO)-term analysis of the CCDC57 and CCDC57 (606-916) proximity interactome for cellular compartment and biological processes revealed significant enrichment of components of the centrosome, satellites and microtubule cytoskeleton as well as their associated functions (Figure 3.5E, 3.6B). In agreement with their distinct cellular localization, components of the centriole duplication were

only enriched in the full-length CCDC57 interactome and components of the microtubule organization were enriched in the CCDC57 (606-916) interactome (Figure 3.5C, 3.5D, 3.6D).

Several of the functional clusters among the proximity interactors of CCDC57 stood out by their association with key centrosome/cilium-mediated cellular processes and their disease links. Cep63 interacts with Cep152 and functions during initiation of centriole duplication, and its mutations were implicated in primary microcephaly (Brown et al., 2013; Sir et al., 2011). KIAA0753 and OFD1 interact and function in cilium assembly and centriole duplication, and their mutations were linked to the oral-facial-digital syndrome (Chevrier et al., 2016; Firat-Karalar et al., 2014; Stephen et al., 2017). PCM1, Cep72 and Cep131 are core centriolar satellite proteins implicated in cilium assembly and cell cycle progression (Hall et al., 2013; Odabasi et al., 2019; Stowe et al., 2012; Wang et al., 2016). Cep192 and components of the HAUS complex function during organization of pericentriolar material (PCM) (Paz and Luders, 2018). To determine which of these proximity interactions can be validated, we performed streptavidin pulldown experiments in HEK293T cells expressing BioID-CCDC57. Cep63, PCM1 and Cep131 pelleted with BioID-CCDC57, but not with BioID itself, confirming the proximity of these proteins to CCDC57 in cells (Figure 3.5F).

Due to the paralogous relationship between Deup1 and Cep63, it is interesting that CCDC57 as a bait identified Cep63 as a proximity partner in this study and was identified as a proximity partner of Deup1 in a previous study (Firat-Karalar et al., 2014). While Deup1 expression is restricted to motile ciliated epithelial cells where it functions in deutorosome-mediated centriole duplication, Cep63 is ubiquitously expressed and functions in canonical centriole duplication (Zhao et al., 2013). Publically available expression data showed that CCDC57, like Cep63, is a ubiquitously expressed protein across different tissues. Therefore, we further focused on the physical relationship between these proteins. Immunoprecipitation experiments in cells expressing GFP-Cep63 confirmed pulldown of endogenous CCDC57 (Figure 3.5G). Additionally, immunoprecipitation and localization experiments in HEK293T cells co-expressing myc-Deup1 and GFP-CCDC57 showed that myc-Deup1 and GFP-CCDC57 interacted and co-localized at the centrosome and the centriolar satellites (Figure 3.6E,

3.6F). Together, these results suggest putative regulatory roles for CCDC57 during initiation of centriole duplication.

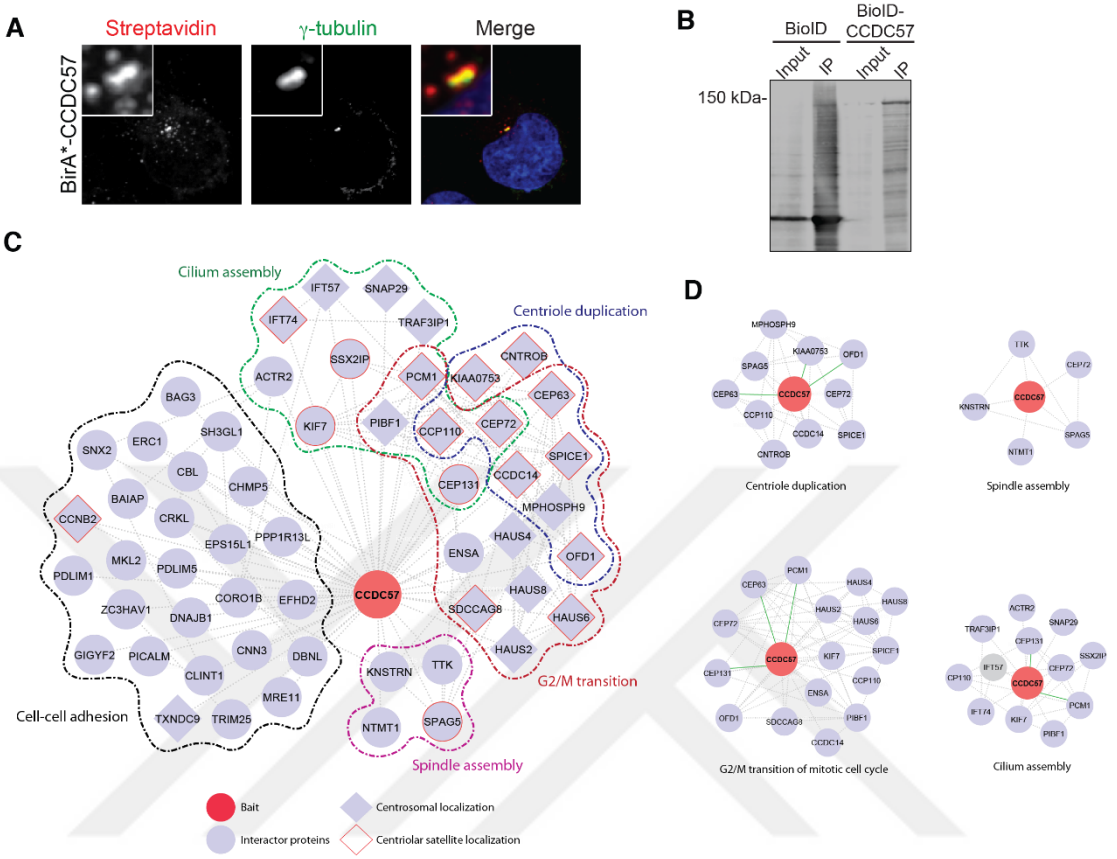

Figure 3.5 CCDC57 has extensive proximity intreactions with Localization, activity and proximity interactors of BirA*-tagged CCDC57 (A) BirA*-CCDC57 stimulates biotinylation at the centrosome and centriolar satellites. U2OS cells were transfected with Myc-BirA*-tagged CCDC57. After 18 h incubation with biotin, cells were fixed and stained for biotinylated proteins with fluorescent streptavidin and centrosome with anti-g-tubulin antibody. DNA was stained with DAPI. Scale bar, 10 µm, insets show 4x enlarged centrosomes. (B) HEK29T cells transfected with BirA* or BirA*-CCDC57 were lysed and biotinylated proteins were precipitated by streptavidin beads. The initial sample (IS) and immunoprecipitated biotinylated proteins (IP) were run on a gel and immunoblotted with fluorescent coupled streptavidin. (C) Mass spectrometry analysis of proximity interactors of Myc-BirA*-CCDC57. Proximity interactors are ranked in the order of their NSAF values (average of three independent experiments) and the first 200 proteins were plotted in the interaction network using Cytoscape. Proteins in diamond shows the ones that localizes to the centrosome, red line around the proteins indicates the proteins that localizes to the centriolar satellites. (D) Sub-interaction networks of CCDC57 based on biological process. Interaction maps are plotted with String database. Green edges indicate the validated interactions in this study (E) GO-enrichment analysis of the first 200 proximity interactors of CCDC57 based on their biological process and cellular compartment. The bar graphs indicate the enrichment of the indicated GO terms. (F) CCDC57 interacts with Cep63 and centriolar satellite proteins Cep131 and PCM1. HEK293T cells were transfected with myc-BirA* or myc-BirA*-CCDC57 and incubated with biotin for 18 h. Complexes were immunoprecipitated with streptavidin beads and co-precipitated proteins were detected with anti-myc, anti-PCM1, anti-Cep63 and anti-Cep131 antibodies. (G) Cep63 interacts with CCDC57. HEK293T cells were transfected with GFP-Cep63, complexes were immunoprecipitated with GFP-Trap beads and co-precipitated proteins were detected with anti-GFP and anti-CCDC57 antibodies.

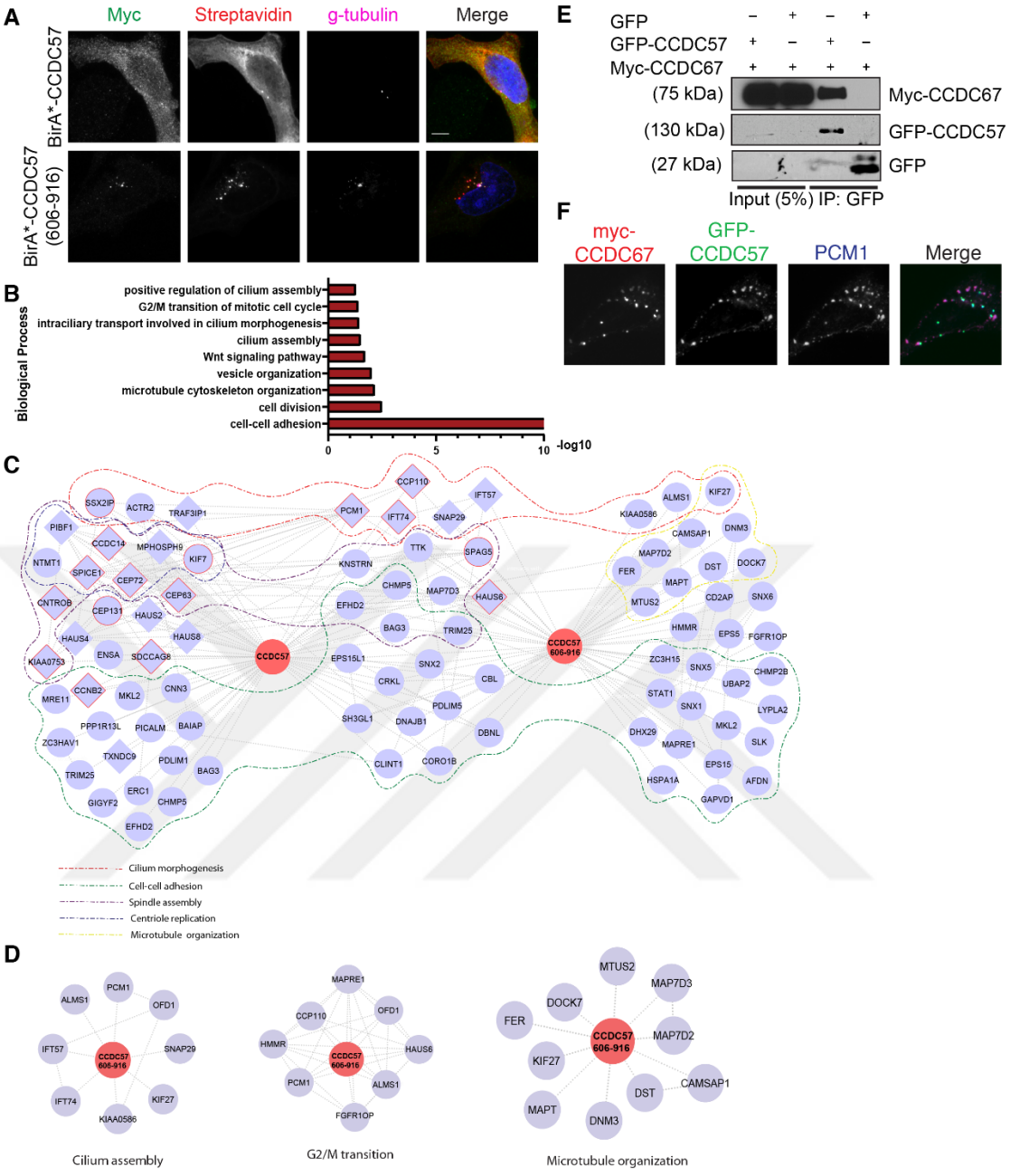
A
Myc
Streptavidin
g-tubulin
Merge
BirA*-CCDC57
BirA*-CCDC57 (606-916)
B
Biological Process
positive regulation of cilium assembly
G2/M transition of mitotic cell cycle
intraciliary transport involved in cilium morphogenesis
cilium assembly
Wnt signaling pathway
vesicle organization
microtubule cytoskeleton organization
cell division
cell-cell adhesion
0
5
10
-log10
C
CCDC57
CCDC57 606-916
Cilium morphogenesis
Cell-cell adhesion
Spindle assembly
Centriole replication
Microtubule organization
D
Cilium assembly
G2/M transition
Microtubule organization
E
GFP
GFP-CCDC57
Myc-CCDC67
(75 kDa)
(130 kDa)
(27 kDa)
Myc-CCDC67
GFP-CCDC57
GFP
Input (5%)
IP: GFP
F
myc-CCDC67
GFP-CCDC57
PCM1
Merge

Figure 3.6. Localization, activity and proximity interactors of BirA*-tagged CCDC57 and CCDC57 (606-916) (A) myc-BirA*-CCDC57 localizes to and stimulates biotinylation the centrosome and centriolar satellites. myc-BirA*-CCDC57 (606-916) localizes to the microtubules and stimulates biotinylation at the centrosome and microtubules. U2OS cells were transfected with Myc-BirA*-tagged CCDC57 and CCDC57 (606-916). After 18 h incubation with biotin, cells were fixed and stained for the fusion proteins with myc antibody, biotinylated proteins with fluorescent streptavidin and centrosome with anti-g-tubulin antibody. DNA was stained with DAPI. Scale bar, 10 μm, (B) GO-enrichment analysis of the first 200 proximity interactors of CCDC57 (606-916) based on their biological process. The bar graphs indicate the enrichment of the indicated GO terms. (C) Mass spectrometry analysis of proximity interactors of Myc-BirA*-CCDC57(606-916) and its comparative analysis with the Myc-BirA*-CCDC57 interactome. The first 200 proximity interactors for both fusions were analyzed for GO enrichment classification into biological processes and overlapping and distinct proteiens identified for different fusions were plotted in the interaction network using Cytoscape. (D) Sub-interaction networks of CCDC57 based on biological process (E, F) CCDC57 localizes and interacts with CCDC67/Deup1. (B) U2OS cells were transfected with GFP-CCDC57 and myc-CCDC67, fixed and stained for GFP, myc, PCM1 and DAPI. (C) HEK293T cells were transfected with GFP-CCDC57 and myc-CCDC67, complexes were immunoprecipitated with GFP-Trap beads and co-precipitated proteins were detected with anti-GFP and anti-myc antibodies.

3.1.5 CCDC57 is required for efficient centriole duplication and cilium assembly

Given its proximity and physical interactions with proteins implicated in centriole duplication, we tested whether CCDC57 is required for canonical centriole duplication and centriole amplification using loss-of-function studies. CCDC57 was efficiently depleted from U2OS cells 86 h after transfection with small interfering RNAs (siRNAs) against CCDC57, as assessed by immunoblotting, immunofluorescence and real-time qPCR experiments (Figure 3.8A-C). We determined the centriole numbers in control and CCDC57-depleted cells by centrin labeling and identified a significant increase in cells that had either one centriole or no centrioles (siControl: %3.3 ± 0.5, siCCDC57: %21.7 ± 3.2, $p< 0.001$) (Figure 3.7A, 3.7B). CCDC57 depletion resulted in mitotic cells with less than two centrioles, suggesting that the duplication defect is not due to failure to progress through the G1/S transition (Figure 3.7A). In agreement with defective canonical centriole duplication, CCDC57 depletion also compromised centriole reduplication during prolonged S phase arrest in U2OS cells. While %61.0 ± 5.8 of control cells had more than four centrioles, %27.7 ± 5.3 of CCDC57-depleted cells had centriole amplification and majority had four or fewer centrioles ($p<0.05$) (Figure 3.7C, 3.7D). The centriole reduplication phenotype was rescued upon

expression of the RNAi-resistant mouse GFP-CCDC57, but not GFP, confirming the specificity of the phenotype (Figure 3.7C, 3.7D).

Cep63 is a key regulator of centriole duplication and centrosome function (Brown et al., 2013; Sir et al., 2011). Because CCDC57 interacts with Cep63, we hypothesized that CCDC57 might function in centriole duplication through regulating centrosomal recruitment of Cep63. To test this, we quantified the centrosomal levels of Cep63 in control and CCDC57-depleted cells and showed that it decreased significantly upon CCDC57 depletion (siControl: 1 ± 0.02, siCCDC57: 0.5 ± 0.02, p value <0.0001) (Figure 3.7E). Immunoblotting of cell extracts indicated that this decrease in centrosomal Cep63 was not due to changes in protein expression upon CCDC57 loss (Figure 3.8B). Analogously, Cep63 depletion resulted in a significant decrease at the centrosomal CCDC57 levels, identifying an interdependent relationship in their centrosomal localization (Figure 3.7F). Cep63 interacts with Cep152 and is required for its recruitment to the proximal end of centrioles. In agreement with this function, CCDC57 depletion also resulted in a significant decrease in its centrosomal levels (siControl: 0.9 ± 0.05, siCCDC57: 0.7 ± 0.06, p value <0.0005) (Figure 3.7G). These results suggest that CCDC57 is required for centrosomal recruitment of Cep63 and Cep152 during centriole duplication.

Centrioles are essential for nucleating the formation of primary cilia. CCDC57 also had proximity interactions with proteins implicated in cilia formation (Figure 3.5). To elucidate functions of CCDC57 in cilium assembly, we depleted CCDC57 in RPE1 cells and quantified the percentage of ciliated cells upon 48 h serum starvation. While control cells ciliated %81 ± 2.6, CCDC57-depleted cells ciliated %48.7 ± 4.6 (p=0.004) (Figure 3.8D, 3.8E). The cilia that formed in CCDC57-depleted cells were shorter in length (siControl: 4.3µm ± 0.1, siCCDC57: 2.9µm ± 0.08, p<0.0001) (Figure 3.8F). Additionally, centriolar satellites that tightly clustered around the basal body of control cells redistributed throughout the cytoplasm upon CCDC57 loss, which was reflected as a significant reduction in the centrosomal PCM1 signal in CCDC57-depleted cells (siControl: 1 ± 0.03, siCCDC57:0.6 ± 0.03 ,p<0.0001) (Figure 3.8G). In agreement, there was also a significant decrease in the amount of centrosomal levels of PCM1 and other centriolar satellites proteins KIAA0753 and Cep131 in CCDC57-

depleted U2OS cells (Figure 3.8H-J). Because centriolar satellites play essential roles during cilium assembly, these results suggest that CCDC57 regulates cilium assembly via its effects on centriolar satellites distribution (Odabasi et al., 2019; Wang et al., 2016).

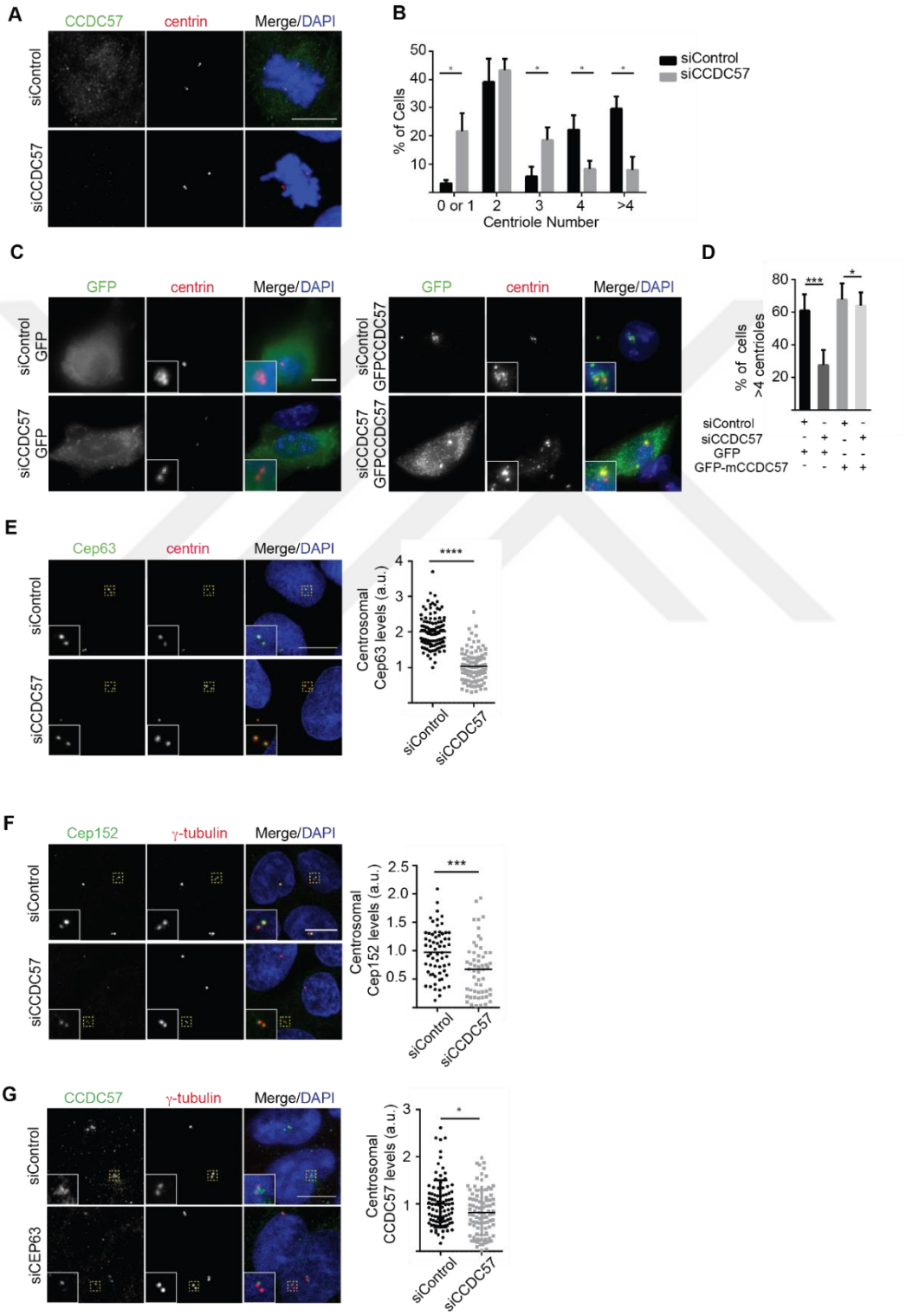

Figure 3.7 CCDC57 is required for centriole duplication and centrosomal recruitment of Cep63 and Cep152. (A) Effect of CCDC57 depletion on centriole duplication. U2OS cells were fixed 86 h after transfection with control siRNA or CCDC57 siRNA, and centriole number was determined by staining for centrin and γ-tubulin. n≥200 cells per experiment. Data represent mean value from four experiments per condition, +/- SEM (**p<0.001, ***p<0.001, ns: not significant) (B) Quantification of centriole duplication experiments in A. n≥150 cells per experiment. Data represent mean value from three experiments per condition, ±SEM (*p<0.05.***p<0.001, ns: not significant) (C) Effect of CCDC57 depletion on centriole amplification during prolonged S phase arrest. U2OS cells were first transfected with control siRNA or CCDC57 siRNA, which was followed by transfection with GFP or GFP-CCDC57. 48 h after hydroxyurea treatment, cells were fixed, stained for GFP and centrin and percentage of cells with more than 4 centrioles. (D) Quantification of centriole overduplication and experiments in C. (E,F) Effect of CCDC57 depletion Cep63 and Cep152 levels at the centrosome. U2OS cells were fixed 86 h after transfection with control siRNA or CCDC57 siRNA, and stained for the indicated proteins. Images represent centrosomes in cells from the same coverslip taken with the same camera settings. Cep63 and Cep152 fluorescence intensity at the centrosome was measured and average means of the levels in control cells were normalized to 1. n=100 cells per experiment. Data represent mean value from two experiments per condition, ± SEM (***p<0.001, ****p<0.0001) (G) Effect of Cep63 depletion on CCDC57 level at the centrosome. U2OS cells were fixed 86 h after transfection with control siRNA or Cep63 siRNA, and stained for the indicated proteins. Images represent centrosomes in cells from the same coverslip taken with the same camera settings. CCDC57 fluorescence intensity at the centrosome was measured and average means of the levels in control cells were normalized to 1. n=100 cells per experiment. Data represent mean value from one experiment per condition, ± SEM (*p<0.05, t-test).

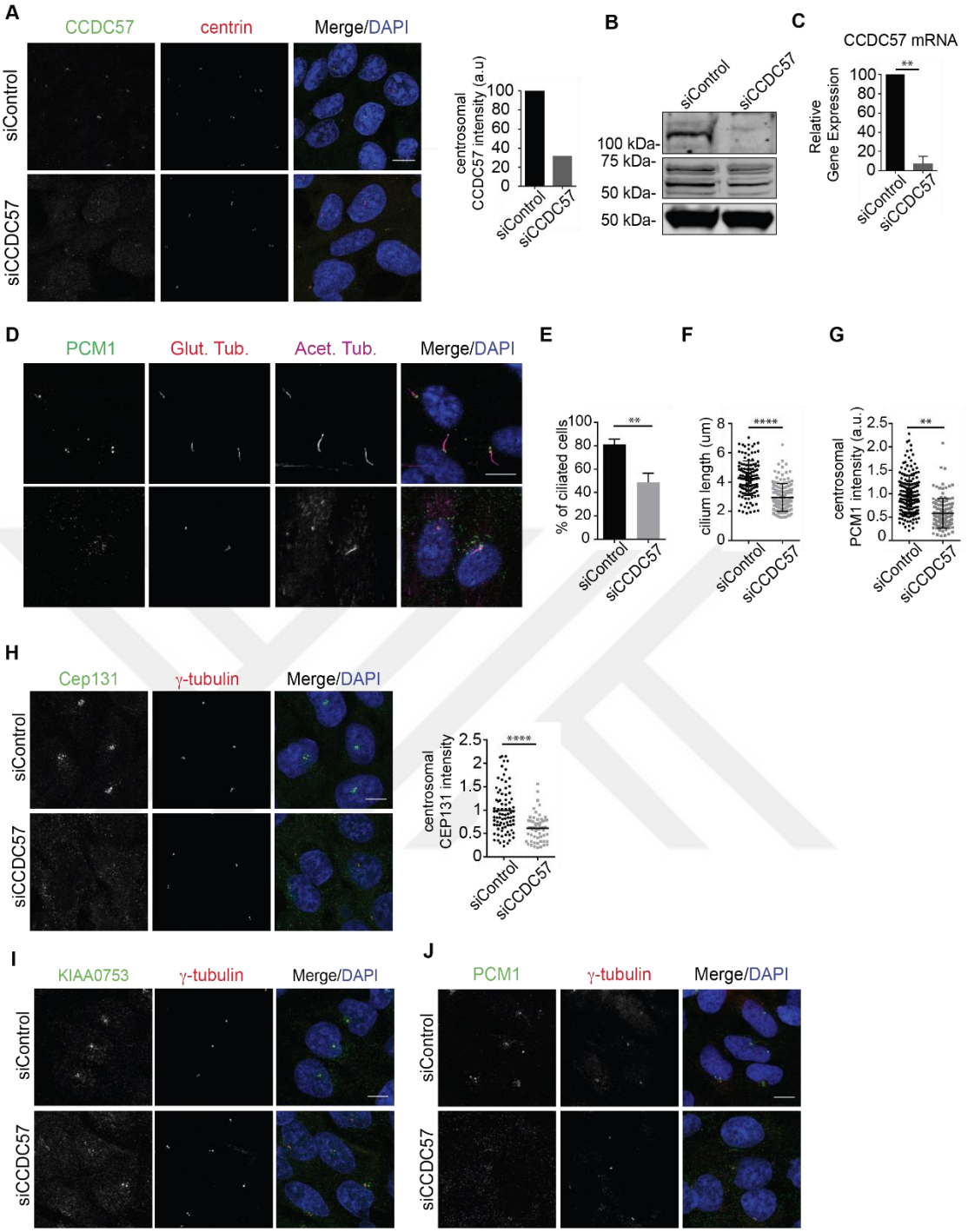
A
CCDC57
centrin
Merge/DAPI
siControl
siCCDC57
centrosomal CCDC57 intensity (a.u)
B
siControl
siCCDC57
100 kDa-
75 kDa-
50 kDa-
50 kDa-
C
CCDC57 mRNA
Relative Gene Expression
D
PCM1
Glut. Tub.
Acet. Tub.
Merge/DAPI
E
% of ciliated cells
F
cilium length (um)
G
centrosomal PCM1 intensity (a.u.)
H
Cep131
γ-tubulin
Merge/DAPI
centrosomal CEP131 intensity
I
KIAA0753
γ-tubulin
Merge/DAPI
J
PCM1
γ-tubulin
Merge/DAPI

Figure 3.8 CCDC57 is required for centriolar satellite distribution and efficient ciliogenesis (A-C) CCDC57 siRNA effectively depletes CCDC57. U2OS cells were transfected with control siRNA or CCDC57 siRNA, and 84 h after transfection (A) fixed and stained for CCDC57, centrin and DAPI. CCDC57 fluorescence intensity at the centrosome was measured and average means of the levels in control cells were normalized to 1. n>50 cells per experiment. Data represent mean values from two experiments, ± SEM (****p<0.0001). (B) cellular extracts were immunoblotted for CCDC57 and tubulin (loading control). (C) CCDC57 mRNA was quantified by qPCR and its fold change is normalized to control cells (=100). Results shown are the mean of two independent experiments±SD (**p<0.01). (D) Effect of satellite loss on cilium formation. Control and CCDC57-depleted RPE1 cells were serum-starved for the 48 h and percentage of ciliated cells was determined by staining for acetylated-tubulin, glutamylated tubulin, PCM1 and DAPI. Scale bar, 10 μm (E) Quantification of ciliogenesis experiments. Results shown are the mean of three independent experiments±SEM (=350 cells/experiment, ****p<0.0001). (F) Effect of CCDC57 depletion on cilium length. Cilium length was determined by staining for acetylated-tubulin and DAPI. (G) Effect of CCDC57 depletion on PCM1 levels at the basal body. PCM1 fluorescence intensity at the basal body was measured and average means of the levels in control cells were normalized to 1. n>80 cells per experiment. Data represent mean values from two experiments, ± SEM (****p<0.0001). (H-J) Effect of CCDC57 depletion on centriolar satellite distribution. U2OS cells were fixed 86 h after transfection with control siRNA or CCDC57 siRNA, and satellite distribution was determined by staining with centriolar satellite markers (H) Cep131, (I) KIAA0753, (J) PCM1, gamma-tubulin and DAPI. Images represent cells from the same coverslip taken with the same camera settings.

3.1.6 CCDC57 is required for mitotic progression

Because CCDC57 binds to microtubules and localizes to spindle microtubules during mitosis, we hypothesized that it might regulate microtubule-mediated cellular processes such as mitotic progression. To test this, we performed time-lapse imaging of control and CCDC57-depleted U2OS cells stably expressing the centriolar marker GFP-centrin 2 and the nuclear marker mCherry-H2B (Figure 3.9A). First, we quantified and compared the mitotic time for the group of control and CCDC57-depleted cells that completed mitosis. Mitotic time was determined as the time from nuclear envelope breakdown to anaphase onset by using mCherry-H2B dynamics as a reference. While the average mitotic time was 38.4±0.9 min for control cells (n=176 mitotic cells out of 1318 cells), it was 51.1±2.4 for CCDC57-depleted cells (n=79 cells out of 1261 cells) (3 independent experiments, p<0.0001) (Figure 3.9B). CCDC57-depleted cells exhibited a higher ratio of mitotic defects such as chromosome misalignment, increased apoptosis, multipolar spindles, and micronuclei (Figure 3.9C-E). Notably, the mitotic index of CCDC57-depleted cells was lower than control cells (siControl: 22.1% ± 1.9, siCCDC57: 11.6% ±1.1, 3 independent experiments, p value=

0.003), suggesting that the increased time these cells spent in mitosis is counterbalanced by an increase in apoptosis or decrease in mitotic entry.

To determine the specific mitotic defects associated with CCDC57 depletion, we quantified the percentage of cells that 1) underwent apoptosis after a long mitotic arrest, 2) had chromosome alignment defects, and 3) had spindle multipolarity and cytokinetic defects associated with concomitant multinucleation. After a prolonged mitotic arrest, %19.8 of CCDC57-depleted cells underwent apoptosis, as assessed by membrane blebbing and DNA fragmentation (control:2% ±2.4, siCCDC57:19.8% ±2.2, $p<0.01$, n=3 experiments) (Figure 3.9C, 3.10B). In agreement with this phenotype, flow cytometry analysis of the asynchronous control and CCDC57-depleted cells showed an increase in the fraction of apoptotic cells upon CCDC57 depletion (Figure 3.9D, 3.10A). Additionally, %25.4 of CCDC57-depleted cells had cytokinetic defects, relative to the %4.6 of control cells (control: 4.6% ±2.3, siCCDC57: 25.4% ±8 $p<0.05$, n=3 experiments) (Figure 3.9C, 3.10B). Majority of these cells initiated cleavage furrow formation that later regressed and resulted in formation of binucleated cells or cells with micronuclei. Finally, %58.7 of CCDC57-depleted cells had chromosome misalignment defects, relative to the %9.1 of control cells (control: 9.1% ±3.4, siCCDC57: 58.7% ±9.0, $p<0.01$, n=3 experiments) (Figure 3.9E, 3.10B).

The mitotic phenotypes associated with CCDC57 depletion might be due to its microtubule-associated functions. To investigate the nature of these functions, we performed microtubule regrowth experiments to determine whether CCDC57 functions in microtubule nucleation and/or anchoring. Microtubule depolymerization in control and CCDC57-depleted cells was induced by one hour nocodazole treatment and cells were then fixed and stained for alpha-tubulin and acetylated-tubulin at different time points after nocodazole washout. Notably, there were higher levels of microtubule regrowth and acetylated microtubules in CCDC57-depleted cells, as evidenced by significant increase in microtubule aster size (Figure 3.9F, 3.9G). Immunoblotting experiments identified a significant increase in the total cellular levels of acetylated tubulin upon CCDC57 loss and no change for alpha-tubulin (Figure 3.9H). To determine whether increase in pericentriolar material underlies the increase in microtubule nucleation in CCDC57-depleted cells, we quantified centrosomal levels of

gamma-tubulin and showed that it was reduced CCDC57-depleted cells (siControl: 0.9± 0.01, siCCDC57: 0.6 ± 0.02, p value <0.0001 (Figure 3.9I). These results together showed that CCDC57 negatively regulates microtubule nucleation, likely through modulating microtubule dynamics but not through an increase pericentriolar material.

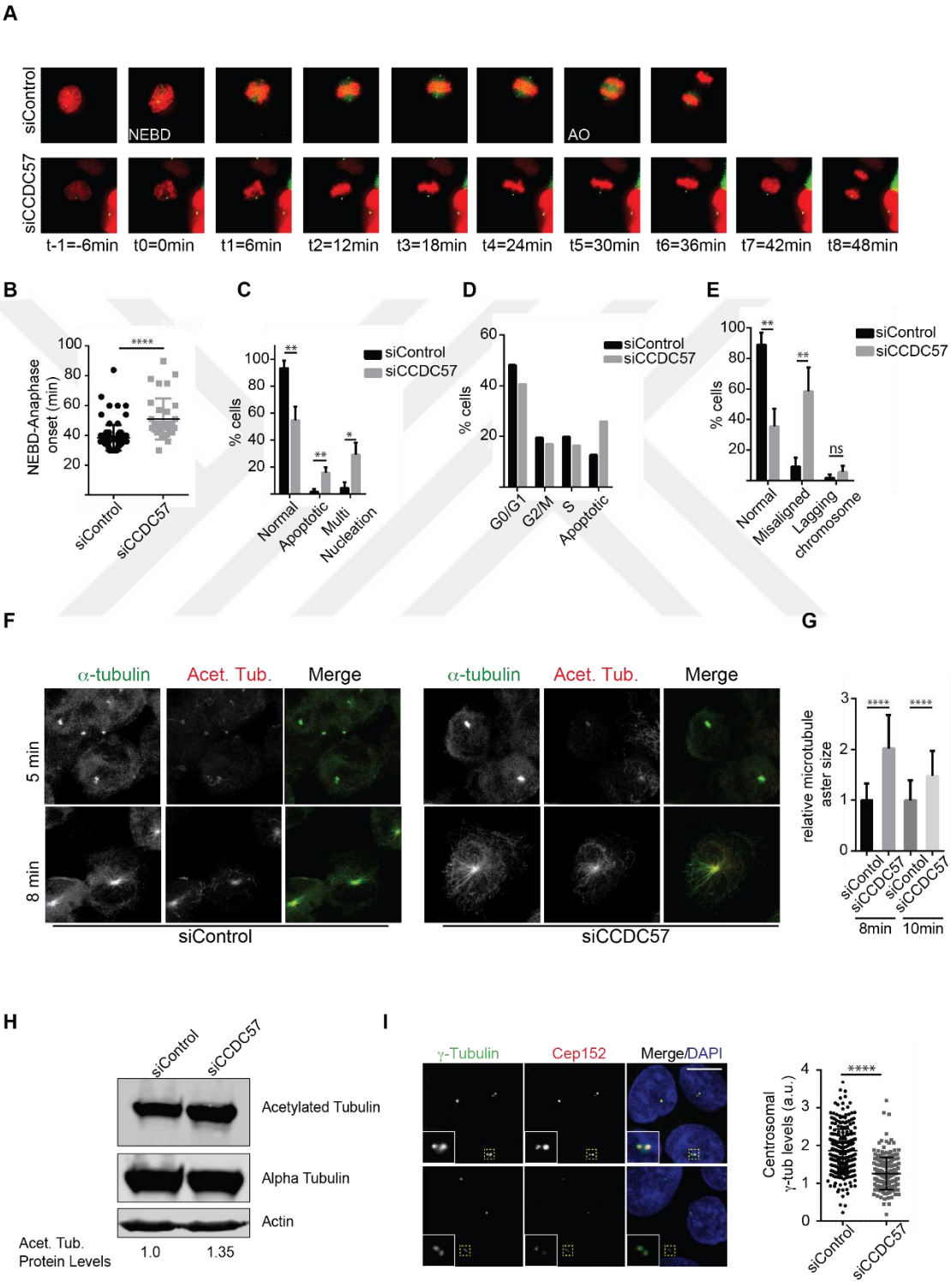

Figure 3.9 CCDC57 is required for timely and faithful mitotic progression (A-D) Effect of CCDC57 depletion on mitotic phenotypes. Control and CCDC57-depleted U2OS cell stably expressing mCherry-H2B and GFP-centrin 2 were imaged every 6 min for 12 h. (A) Representative still frames from time-lapse experiments were shown. (B) Mitotic time was quantified as the time interval from nuclear envelope breakdown (NEBD) to anaphase onset. n>50 mitotic cells per experiment. Data represent mean ± SEM of four independent experiments (****p<0.0001). (C) Percentage of control and CCDC57-depleted mitotic cells were quantified based on cells that completed mitosis, cells that underwent apoptosis and cells with cytokinetic defects. n>50 cells per experiment. Data represent mean ± SEM of three independent experiments (**p<0.01, ns: not significant). (D) Effect of CCDC57 depletion on percentage of cells in different cell cycle phases. Control and CCDC57-depleted cells fixed and their DNA content was assessed by flow cytometry. (E) Percentage of control and CCDC57-depleted mitotic cells were quantified based on chromosome alignment and segregation phenotypes that included normal, misaligned and lagging chromosomes. n>50 cells per experiment. Data represent mean ± SEM of three independent experiments (**p<0.01, ns: not significant). (F) Effect of CCDC57 depletion on microtubule nucleation. Control and CCDC57-depleted U2OS cells were treated with DMSO or 10 μg/ml nocodazole for 1 h. After microtubule depolymerization, cells were washed, incubated with media for the indicated times, fixed and stained for alpha-tubulin, acetylated tubulin and DAPI. Images represent cells from the same coverslip taken with the same camera settings. Scale bars = 10 μm. (G) Microtubule aster size was quantified 8 min and 10 min after nocodazole washout. n=50 cells per experiment. Data represent mean ± SEM of two independent experiments (***p<0.001). (H) Effect of CCDC57 depletion on cellular abundance of acetylated tubulin. U2OS cells were transfected with control or CCDC57 siRNAs, and 86 h after transfection cell extracts were immunoblotted for alpha-tubulin, acetylated tubulin and actin (loading control). (I) Effect of CCDC57 depletion on gamma-tubulin level at the centrosome. U2OS cells were fixed 84 h after transfection with control siRNA or CCDC57 siRNA, and stained for gamma-tubulin, Cep152 and DAPI. Images represent centrosomes in cells from the same coverslip taken with the same camera settings. Gamma-tubulin fluorescence intensity at the centrosome was measured and average means of the levels in control cells were normalized to 1. n>100 cells per experiment. Data represent mean value from two experiments, ± SEM

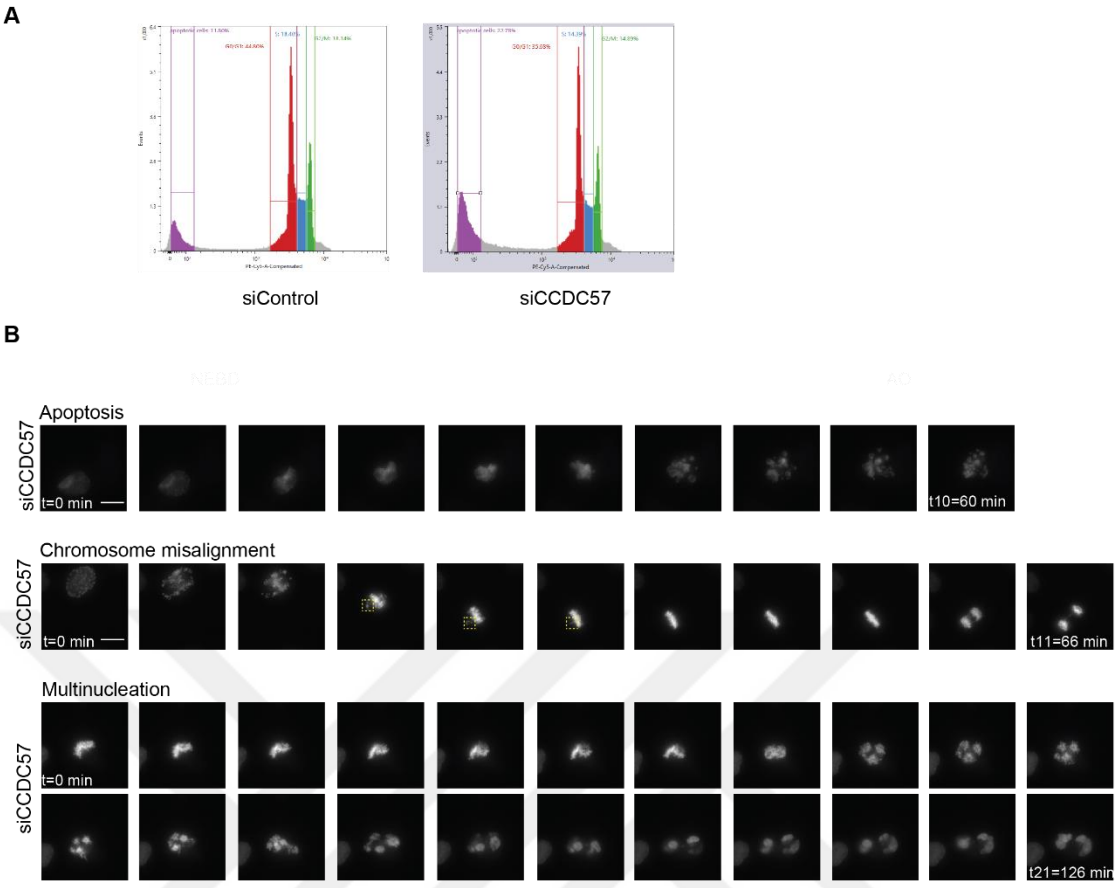

Figure 3.10 CCDC57 is required for timely and faithful mitotic progression (A) Effect of CCDC57 depletion on cell cycle progression. Flow cytometry analysis of control or CCDC66-depleted cells. Control and CCDc-57depleted U2OS cells were harvested and fixed in 70% ethanol, washed with PBS and stained with 40 µg/ml propidium iodide and 10 µg/ml RNaseA. DNA content was assessed by flow cytometry. (B) Effect of CCDC57 depletion on mitotic phenotypes. Representative still frames from time-lapse experiments taken at 6 min intervals were shown to represent apoptosis, misaligned chromosomes and multinucleation Scale bar, 8 µm

3.2 Discussion

In this study, we characterized CCDC57 as a new component of centrosomes, centriolar satellites and microtubules. CCDC57 forms a complex with Cep63 and centriolar satellite proteins and functions in initiation of centriole duplication through regulating Cep63 and Cep152 targeting to the centrosome. Additionally, CCDC57 localizes to spindle microtubules during mitosis and is required for microtubule nucleation, mitotic progression and chromosome alignment. Our results provide new insight into the molecular defects that underlie the pathogenesis of primary microcephaly and cancer.

Characterization of CCDC57 deletion mutants for their cellular localization showed that CCDC57 is targeted centrosomes and microtubules through distinct regions at its N- and C-terminus. The N-terminal centrosomal targeting region is comprised of three coiled-coil domains, which likely mediates its dimerization with other centrosome proteins. In agreement, we showed that Cep63 is required for centrosomal targeting of CCDC57. In contrast to the centrosomal targeting domain, the C-terminal microtubule targeting region has no identifiable domains. The stretches of amino acids conserved in CCDC57 orthologues were neither enriched in basic amino acids nor had homology to other microtubule-biding proteins, including the centrosomal proteins like Cep120, Cep135, CPAP, Mdm1 and CCSAP that were also identified as microtubule-associated proteins (Backer et al., 2012; Carvalho-Santos et al., 2012; Hsu et al., 2008; Lin et al., 2013b; Van de Mark et al., 2015). Future in vitro microtubule sedimentation, polymerization and dynamics experiments with purified CCDC57 and its fragments are required to elucidate on the nature of relationship between CCDC57 and microtubules and these studies will inform the likely microtubule-mediated mitotic functions of CCDC57.

Given that the localization affinities are separated within CCDC57, we propose that its dual functions in centriole duplication and mitotic progression is mediated by centrosomal and microtubule-targeting regions, respectively. CCDC57 interacts with Cep63 and is required for its centrosomal recruitment, which together indicates that their compromised interaction is the likely underlying mechanism for centriole

duplication defects associated with CCDC57 loss. Overexpression of CCDC57 N-terminal centrosome targeting region resulted in formation of aggregates that recruited Cep63, identifying this part of CCDC57 as the required region for centriole duplication. Moreover, full-length CCDC57, but not CCDC57 (606-916), had specific proximity interactions with centriole duplication proteins such as Cep63. Finally, we found that a subset of CCDC57-depleted cells with mitotic defects did not have reduced centriole numbers and this data shows that failure in centriole duplication was not the only cause of mitotic defects in these cells. Therefore, mitotic functions of CCDC57 are likely mediated in part or fully by its microtubule-associated activities.

How does CCDC57 regulate microtubules to function during mitotic progression and fidelity? Microtubule regrowth experiments identified CCDC57 as a suppressor of microtubule nucleation and acetylation. Increase in microtubule nucleation was not due to increase in the amount of pericentriolar material, which is different than the inhibitory mechanisms reported for other centrosome proteins such as the daughter centriole protein Cep120 (Betleja et al., 2018). A possible mechanism for this inhibition is that CCDC57 cooperates or competes with other microtubule-associated proteins to regulate microtubule nucleation and stability. The proximity interactome of CCDC57 (606-916) microtubule-targeting region identified MAPs including CAMSAP1 and MAP7D3 which might be the potential candidates (Hueschen et al., 2017; Yadav et al., 2014). Despite these intriguing possibilities, we would like to highlight that it is also possible that the mitotic defects associated with CCDC57 depletion are a consequence of defective Cep63 centrosomal recruitment and centriole duplication. In fact, analogous to CCDC57, loss of Cep63 were shown to cause increased apoptosis, mitotic errors and delays (Marjanovic et al., 2015). In addition to further dissecting in vitro and in vivo effects of CCDC57 on microtubules, rescue or dominant-negative studies will be required to correlated function with structural domains.

CCDC57 has extensive proximity interactions with centrosome proteins implicated in centrosome-mediated cellular processes. Proximity and physical interactions of CCDC57 with Cep63 and its function in centriole duplication together identify CCDC57 as part of the Cep63-Cep152 functional module required for initiation of centriole duplication. While our data shows that defects in the centrosomal recruitment of

Cep63 and Cep152 in part underlies the centriole duplication defects associated with CCDC57 depletion, how this regulation is imparted at the molecular level is not known. Analogous to the functional relationship between Cepe63 and Cep152, it could be a simple targeting mechanism where CCDC57 and Cep63 provide binding sites for each other at the centrosome (Sir et al., 2011). However, unlike Cep63 and Cep152, CCDC57 and Cep63 only partially co-localizes at the proximal end of the centriole. The apparent lack of co-localization might be due to their transient interaction at the centrosome that cannot be detected by co-localization experiments or their interaction at the cytosol that regulates their centrosomal targeting. In fact, like Cep63, CCDC57 localizes to and forms a complex with centriolar satellites, suggesting that it might regulate centrosomal Cep63-targeting via satellites. In agreement with this model, centriolar satellite proteins including KIAA0753 were shown to mediate Cep63 targeting to centrosomes (Firat-Karalar et al., 2014; Kodani et al., 2015). Given the interaction between CCDC57 and PCM1, it is likely that CCDC57 cooperates with satellite proteins such as KIAA0753 to regulate centrosomal targeting of Cep63.

In previous work, we previously identified CCDC57 as a proximity interactor of the Cep63 paralogue CCDC67/Deup1, which functions in deuterosome-mediated centriole duplication in multiciliated epithelial cells (MCCs) (Firat-Karalar et al., 2014; Zhao et al., 2013). In reciprocal BioID experiments, we did not identify Deup1 as a proximity partner for CCDC57, which is due to the restricted Deup1 expression in MCCs. Of note, co-immunoprecipitation and co-localization experiments in cells ectopically expressing GFP-CCDC57 and myc-Deup1 demonstrated that these proteins can localize and interact with each other. Given that Cep63-Deup1 paralogous pair are critical regulators of centriole duplication in MCCs and Deup1 is the only deutorosome-specific protein identified to date, future localization and loss-of-function studies in MCCs are required to dissect the functions and mechanisms of CCDC57 in these cells. These studies have the potential to identify a new component to the centriole duplication pathways in MCCs, which have remained poorly characterized.

Almost all proteins mutated in primary microcephaly are components of the centrosome that function in centriole duplication and spindle assembly, which highlights the crucial roles imparted by centrosomes during neurodevelopment as well

as the importance of centriole number control. The results of our study places CCDC57 in the context of functional modules associated with microcephaly, in particular the Cep63-Cep152 module that ensures efficient centriole duplication and faithful mitotic progression (Brown et al., 2013; Marjanovic et al., 2015; Sir et al., 2011). Although no microcephaly patient mutations have been reported for CCDC57 to date, our data identify CCDC57 as a candidate microcephaly gene and targeted searches for CCDC57 mutations in microcephaly patients by whole exome sequencing is required to address this possibility. Additionally, loss-of-function studies in animal models and mini brain organoids will be required to determine whether, and if so, to what step of neurodevelopment CCDC57 contributes

4 MATERIALS AND METHODS

Cell culture and transfection

Human telomerase immortalized retinal pigment epithelium cells (hTERT-RPE1, ATCC, CRL-4000) were cultured with Dulbecco's modified Eagle's Medium DMEM/F12 50/50 medium (Pan Biotech, Cat. # P04-41250) supplemented with 10% Fetal Bovine Serum (FBS, Life Technologies, Ref. # 10270-106, Lot # 42Q5283K) and 1% penicillin-streptomycin (Gibco, Cat. # 1540-122). Human embryonic kidney (HEK293T, ATCC, CRL-3216) and osteosarcoma epithelial (U2OS, ATCC, HTB-96) cells were cultured with DMEM medium (Pan Biotech, Cat. # P04-03590) supplemented with 10% FBS and 1% penicillin-streptomycin. All cell lines were authenticated by Multiplex Cell Line Authentication (MCA) and were tested for mycoplasma by MycoAlert Mycoplasma Detection Kit (Lonza). RPE1 and U2OS cells were transfected with the plasmids using Lipofectamine 2000 according to the manufacturer's instructions (Thermo Fisher Scientific). HEK293T cells were transfected with the plasmids using 1 μg/μl polyethylenimine, MW 25 kDa (PEI, Sigma-Aldrich, St. Louis, MO). For serum starvation experiments, RPE1 cells were washed twice with PBS and incubated with DMEM/F12 50/50 supplemented with 0.5% FBS and 1% penicillin-streptomycin for the indicated times. For microtubule depolymerization experiments, cells were treated with 10 μg/ml nocodazole (Sigma-Aldrich, Cat. #M1404) or vehicle (dimethyl sulfoxide) for one hour at 37°C. For microtubule regrowth experiments, cells were washed 3X with PBS after microtubule depolymerization, incubated in warm media for the indicated times, fixed and stained. IMCD3 cells stably expressing LAP-CCDC57, LAP-CCDC57 (1-502) and LAP-CCDC57 (503-916) were generated by cotransfecting IMCD3 Flip-in cells with pEF5.FRT.LAP expression vectors and pOG44.

Plasmids and Cloning

Full-length cDNAs of Homo sapiens CCDC57 (GenBank accession no. 284001) and Mus musculus (CCDC57 (GenBank accession no. 71276) were obtained from Open Biosystems. The ORF of CCDC57 was amplified by PCR and cloned into pDONR221 using the Invitrogen Gateway system. Subsequent Gateway recombination reactions

using pCS2+6xMyc DEST, pcDNA-DEST47, pEF5/FRT/LAPN-DEST, pDEST-myc-BirA* and pLVPT2-GFP-N1 were used to generate GFP-CCDC57, LAP-CCDC57, BioID-CCDC57 and pLVPT2-GFP-CCDC57. Deletions constructs of CCDC57 were made by PCR amplification of the indicated regions. PCR products were cloned into pDONR221 and gateway recombination reactions using pcDNA-DEST47, pLVPT2-GFP-N1 and pEF5/FRT/LAPN-DEST were used to produce GFP, Lenti-GFP and LAP-tagged deletion constructs. pEGFP-C1-Cep63 (GenBank/EMBL/DDBJ accession no. NM_001042383.1) was used for Cep63 expression. pLVPT2-GFP-N1 were used to generate GFP-CCDC57, LAP-CCDC57, BioID-CCDC57 and pLVPT2-GFP-CCDC57. Deletions constructs of CCDC57 were made by PCR amplification of the indicated regions. PCR products were cloned into pDONR221 and gateway recombination reactions using pcDNA-DEST47, pLVPT2-GFP-N1 and pEF5/FRT/LAPN-DEST were used to produce GFP, Lenti-GFP and LAP-tagged deletion constructs

Antibodies

Antibodies used for immunofluorescence were rabbit anti-CCDC57 (HPA023315; Merck), mouse anti-γ-tubulin (GTU-88; T5326; Merck) at 1:4000, rabbit antiGFP (rabbit anti-GFP at 1.5 μg/ml (as previously described in (Hatch et al., 2010), rabbit anti-Myc (sc-789; Santa Cruz Biotechnology) at 1:1000, mouse anti-Centrin3 (M01-3E6; Abnova) at 1:750, mouse anti α-tubulin (DM1A; ab40742; Abcam), mouse anti-Rootletin (sc-374056; Santa Cruz Biotechnology) at 1:500, mouse anti-Myc (9e10; M4439; Sigma-Aldrich) at 1:500 and mouse anti-polyglutamylated tubulin (GT335; AG-20B-0020-C100; Adipogen) at 1:2000. Antibodies used for western blotting were rabbit anti-CCDC57 (HPA023344; Merck), rabbit anti-GFP at 0.15 μg/ml (as previously described in (Hatch et al., 2010)), mouse anti- beta actin (60008-1-Ig; Proteintech) at 1:10.000, rabbit anti-GAPDH (10494-1-AP, Proteintech) at 1:10.000, mouse anti-γ-tubulin (GTU-88; T5326; Merck) at 1:2000

APPENDIX

RNAi and rescue experiments

CCDC57 was depleted using an siRNA with the sequence 5'-AGCAGGACAUUGAAAGGUAtt-3' ordered from Thermo Fisher Scientific. For depletion of Cep63, previously characterized siRNA 5'-AGUCCAGCGAUUUCUGACGUU-3' were custom-ordered from Dharmacon(Brown et al., 2013). Control siRNA#1 (Dharmacon, Cat. # D-001210-02-05) was used as control. Cells were seeded onto coverslips at 70% confluency and transfected with 50 nM of siRNA in two sequential transfections using Lipofectamine RNAiMAX (Life Technologies, Ref. # 13778-150, Lot # 2009103) in OPTI-MEM (Life Technologies, Cat. # 31985062). Depletion of proteins was confirmed 86 h after transfection by immunofluorescence and immunoblotting. For rescue experiments, cells were transfected with control and CCDC57 siRNAs using Lipofectamine RNAiMax (Thermo Fisher Scientific) followed by transfection with GFP or GFP-mCCDC57 using Lipofetamine 2000. 86 h posttransfection with the siRNAs, cells were fixed and stained.

Immunofluorescence, antibodies and microscopy

Cells were grown on coverslips, washed twice with PBS and fixed in either ice cold methanol at -20°C for 10 minutes or 4% PFA in PBS for indirect immunofluorescence. After rehydration in PBS, cells were blocked with 3% BSA (Capricorn Scientific, Cat. # BSA-1T) in PBS + 0.1% Triton X-100 followed by incubation with primary antibodies in blocking solution for 1 hour at room temperature. Cells were washed three times with PBS and incubated with secondary antibodies and DAPI (Thermo Scientific, cat#D1306) at 1:2000 for 45 minutes at room temperature. Following three washes with PBS, cells were mounted using Mowiol mounting medium containing N-propyl gallate (Sigma-Aldrich). Primary antibodies used for immunofluorescence were mouse anti-acetylated tubulin (clone 6-11B, 32270, Thermo Fischer) at 1:10000, mouse anti gamma tubulin (Sigma, clone GTU-88, T5326) at 1:1000, mouse anti GFP (3E6) 1:750, mouse anti alpha tubulin (Sigma, DM1A) at 1:1000, rabbit anti CEP152 (Bethyl, A302-480A) at 1:500, rabbit anti-KIAA0753 (Sigma, HPA023494) at 1:1000, rabbit anti-Cep131 (Proteintech, 25757-1-AP) at 1:1000, rabbit anti-CCDC57 (Sigma, HPA023344 and HPA023315) at 1:1000 and mouse anti-centrin 3 (Abnova, clone 3E6) at 1:1000.

APPENDIX

Rabbit anti-PCM1 and anti-GFP antibodies were generated and used for immunofluorescence as previously described (Firat-Karalar et al., 2014). Secondary antibodies used for immunofluorescence experiments were AlexaFluor 488-, 568- or 633-coupled (Life Technologies) and they were used at 1:2000. Biotinylated proteins were detected with streptavidin coupled to Alexa Fluor 594 (1:500; Life Technologies).

Time lapse live imaging was performed with Leica DMi8 inverted fluorescence microscope equipped with an incubation chamber. For cell cycle experiments, asynchronous cells were imaged at 37°C with 5% CO2 with a frequency of 6 minutes per frame with 1.5 µm step size and 12 µm stack size in 1024x1024 pixel format at a specific position using HC PL APO CS2 40x 1.3 NA oil objective. For centrosomal protein level quantifications, images were acquired with Leica DMi8 inverted fluorescent microscope with a stack size of 8 µm and step size of 0.5 µm in 1024x1024 format using HC PL APO CS2 63x 1.4 NA oil objective. Higher resolution images were taken by using HC PL APO CS2 63x 1.4 NA oil objective with Leica SP8 confocal microscope. For 3D-SIM analysis of CCDC57, cells were imaged on an inverted Nikon Ti-E microscope using 100X 1.45 NA oil objective at the Washington Universtiy Center for Cellular Imaging.

Quantitative immunofluorescence for CCDC57, Cep63, Cep152, CEP131(AZI1), KIAA0753 and PCM1 was performed by acquiring a z-stack of control and depleted cells using identical gain and exposure settings. The maximum-intensity projections were assembled from z-stacks. The centrosome region for each cell were defined by staining for a centrosomal marker including gamma-tubulin and centrin. The region of interest that encompassed the centrosome was defined as a circle 3.5-µm2 area centered on the centrosome in each cell. Total pixel intensity of fluorescence within the region of interest was measured using ImageJ (National Institutes of Health, Bethesda, MD) (Schneider et al., 2012). Background subtraction was performed by quantifying fluorescence intensity of a region of equal dimensions in the area proximate to the centrosome. Statistical analysis was done by normalizing these values to their mean.

Primary cilium formation was assessed by counting the total number of cells, and the number of cells with primary cilia, as detected by DAPI and acetylated tubulin staining,

respectively. Ciliary length was measured using acetylated tubulin as the ciliary length marker. All values were normalized relative to the mean of the control cells (=1). As for quantification of microtubule regrowth phenotypes, microtubule aster size was determined by drawing a circular region from the centrosome to the distal end of the longest microtubule tip in each cell.

Cell lysis and immunoblotting

Cells were lysed in 50 mM Tris (pH 7.6), 150 mM NaCl, 1% Triton X-100 and protease inhibitors for 30 min at 4°C followed by centrifugation at 15.000 g for 15 min. The protein concentration of the resulting supernatants was determined with the Bradford solution (Bio-Rad Laboratories, CA, USA). For immunoblotting, equal quantities of cell extracts were resolved on SDS-PAGE gels, transferred onto nitrocellulose membranes, blocked with TBST in 5% milk for 1 hour at room temperature. Blots were incubated with primary antibodies diluted in 5% BSA in TBST overnight at 4°C, washed with TBST three times for 5 minutes and blotted with secondary antibodies for 1 hour at room temperature. After washing blots with TBST three times for 5 minutes, they were visualized with the LI-COR Odyssey® Infrared Imaging System and software at 169 µm (LI-COR Biosciences). Primary antibodies used for immunoblotting were rabbit anti PCM1 (Proteintech, 19856-1-AP) at 1:500, mouse anti beta-actin (Proteintech, 60008-1-Ig) at 1:10000, mouse anti alpha-tubulin (Sigma, DM1A) at 1:5000, anti-CCDC57 (Sigma, HPA023344 and HPA023315) at 1:1000, anti-c-Myc (Santa Cruz Biotechnology, clone 9E10) and mouse anti- acetylated tubulin (clone 6-11B, 32270, Thermo Fischer) at 1:5000. anti-PCM1 and anti-GFP antibodies were generated and used for immunobloting as previously described (Firat-Karalar et al., 2014). Secondary antibodies used for western blotting experiments were IRDye680- and IRDye 800-coupled and were used at 1:15000 (LI-COR Biosciences).

Immunoprecipitation

HEK293T cells were transfected with the indicated constructs. 24 h after transfection, cells were washed with PBS, lysed in IP buffer (50 mM Tris-HCl pH 7.4, 260 mM NaCl, 2.27 mM KCl, 1.25 mM KH2PO4, 6.8 mM Na2HPO4, 1% NP-40) supplemented with protease inhibitors (10 µg/ml Leupeptin, Pepstatin and Chymostatin, 1 mM PMSF, 10

µg/ml Aprotinin), tumbled at 4°C for 45 min, and centrifuged at 13.000 R.P.M. for 15 minutes. Insoluble material was pelleted, and supernatant was incubated with GFP-Trap agarose beads (Chromotek, GTA#10) at 4°C for 45 min. Beads were washed in lysis buffer, eluted in sample buffer, and ran on SDS-PAGE gels.

Biotin-streptavidin affinity purification

For the BioID experiments, HEK293T cells were transfected with BirA*-tagged proteins. 24 h post-transfection, transfected cells were supplemented with 50 µM biotin and incubated a further 18 h. After transfection with BirA*-tagged proteins and biotin treatment, cells were directly lysed in lysis buffer. An equal volume of 4 °C 50 mM Tris (pH 7.4) was added to the extracts and insoluble material was pelleted. Soluble materials from whole cell lysates and centrosome enriched extracts were incubated with Streptavidin agarose beads (Thermo Scientific) overnight. Beads were collected and washed twice in wash buffer 1 (2% SDS in dH2O), once with wash buffer 2 (0.2% deoxycholate, 1% Triton X-100, 500 mM NaCl, 1 mM EDTA, and 50 mM Hepes, pH 7.5), once with wash buffer 3 (250 mM LiCl, 0.5% NP-40, 0.5% deoxycholate, 1% Triton X-100, 500 mM NaCl, 1 mM EDTA and 10 mM Tris, pH 8.1) and twice with wash buffer 4 (50 mM Tris, pH 7.4, and 50 mM NaCl). 10% of the sample was reserved for Western blot analysis and 90% of the sample to be analyzed by mass spectrometry was washed twice in 50 mM NH4HCO3.

Mass spectrometry and data analysis

Mass spectrometry analysis was done as described previously with the following change (Firat-Karalar et al., 2014): The MS/MS spectra were searched with the ProLuCID algorithm against the Uniprot human database (downloaded on 03202014). For each BioID experiment data were derived from two biological replicates. Control data were derived from mock-transfected and BirA*- transfected HEK293T cells. To compare data across different runs and assess the abundance of each proximity partner, we applied the normalization of spectral counts (Zybailov et al., 2006). Individual spectral count values were normalized against the sum of all spectral counts for a particular run, resulting in normalized spectral abundance factor (NSAF). To distinguish the nonspecific interactors, we calculated the ratio of the NSAF of each

identified protein to the NSAF of the corresponding proteins in the control datasets. A protein was considered a contaminant if the ratio was smaller than 2.5. For analysis of the data from two independent BioID experiments, we only accounted for the proteins that were identified in both replicates. Interaction maps were drawn using Cytoscape. GO-enrichment analysis was done using DAVID Functional Annotation Bioinformatics Microarray Analysis. For generating sub-interaction maps for specific functional clusters, we performed STRING analysis for the selected set of proteins.

Statistical tests

Statistical results, average and standard deviation values were computed and plotted by using Prism (GraphPad, La Jolla, CA). Two-tailed t-tests and ANOVA were applied to compare the statistical significance of the measurements. Error bars reflect SEM. Following key is followed for asterisk placeholders for p-values in the figures: *P < 0.05, **P < 0.01, ***P < 0.001, **** P < 0.0001

References

Anderson, R. G. and R. M. Brenner (1971). "The formation of basal bodies (centrioles) in the Rhesus monkey oviduct." J Cell Biol **50**(1): 10-34.

Arquint, C., A.M. Gabryjonczyk, S. Imseng, R. Bohm, E. Sauer, S. Hiller, E.A. Nigg, and T. Maier. 2015. STIL binding to Polo-box 3 of PLK4 regulates centriole duplication. eLife. 4.

Arquint, C., and E.A. Nigg. 2016. The PLK4-STIL-SAS-6 module at the core of centriole duplication. Biochem Soc T. 44:1253-1263.

Azimzadeh, J. (2014). "Exploring the evolutionary history of centrosomes." Philos Trans R Soc Lond B Biol Sci **369**(1650).

Azimzadeh, J., and W.F. Marshall. 2010. Building the centriole. Curr Biol. 20:R816-825.

Backer, C.B., J.H. Gutzman, C.G. Pearson, and I.M. Cheeseman. 2012. CSAP localizes to polyglutamylated microtubules and promotes proper cilia function and zebrafish development. Mol Biol Cell. 23:2122-2130.

Bahe, S., Y. D. Stierhof, C. J. Wilkinson, F. Leiss and E. A. Nigg (2005). "Rootletin forms centriole-associated filaments and functions in centrosome cohesion." J Cell Biol **171**(1): 27-33.

Balczon, R., L. Bao and W. E. Zimmer (1994). "PCM-1, A 228-kD centrosome autoantigen with a distinct cell cycle distribution." J Cell Biol **124**(5): 783-793.

Baldauf, S. L., A. J. Roger, I. Wenk-Siefert and W. F. Doolittle (2000). "A kingdom-level phylogeny of eukaryotes based on combined protein data." Science **290**(5493): 972-977.

Barenz, F., D. Mayilo and O. J. Gruss (2011). "Centriolar satellites: busy orbits around the centrosome." Eur J Cell Biol **90**(12): 983-989.

Basto, R., J. Lau, T. Vinogradova, A. Gardiol, C. G. Woods, A. Khodjakov and J. W. Raff (2006). "Flies without centrioles." Cell **125**(7): 1375-1386.

Bauer, M., F. Cubizolles, A. Schmidt and E. A. Nigg (2016). "Quantitative analysis of human centrosome architecture by targeted proteomics and fluorescence imaging." EMBO J **35**(19): 2152-2166.

Bazzi, H. and K. V. Anderson (2014). "Acentriolar mitosis activates a p53-dependent apoptosis pathway in the mouse embryo." Proc Natl Acad Sci U S A **111**(15): E1491-1500.

Beroukhim, R., C. H. Mermel, D. Porter, G. Wei, S. Raychaudhuri, J. Donovan, J. Barretina, J. S. Boehm, J. Dobson, M. Urashima, K. T. Mc Henry, R. M. Pinchback, A. H. Ligon, Y. J. Cho, L. Haery, H. Greulich, M. Reich, W. Winckler, M. S. Lawrence, B. A. Weir, K. E. Tanaka, D. Y. Chiang, A. J. Bass, A. Loo, C. Hoffman, J. Prensner, T. Liefeld, Q. Gao, D. Yecies, S. Signoretti, E. Maher, F. J. Kaye, H. Sasaki, J. E. Tepper, J. A. Fletcher, J. Tabernero, J. Baselga, M. S. Tsao, F. Demichelis, M. A. Rubin, P. A. Janne, M. J. Daly, C. Nucera, R. L. Levine, B. L. Ebert, S. Gabriel, A. K. Rustgi, C. R. Antonescu, M. Ladanyi, A. Letai, L. A. Garraway, M. Loda, D. G. Beer, L. D. True, A. Okamoto, S. L. Pomeroy, S. Singer, T. R. Golub, E. S. Lander, G. Getz, W. R. Sellers and M. Meyerson (2010). "The landscape of somatic copy-number alteration across human cancers." Nature **463**(7283): 899-905.

APPENDIX

Betleja, E., R. Nanjundappa, T. Cheng, and M.R. Mahjoub. 2018. A novel Cep120-dependent mechanism inhibits centriole maturation in quiescent cells. eLife. 7.

Bettencourt-Dias, M. and D. M. Glover (2007). "Centrosome biogenesis and function: centrosomics brings new understanding." Nat Rev Mol Cell Biol **8**(6): 451-463.

Bettencourt-Dias, M., F. Hildebrandt, D. Pellman, G. Woods, and S.A. Godinho. 2011. Centrosomes and cilia in human disease. Trends Genet. 27:307-315.

Bettencourt-Dias, M., A. Rodrigues-Martins, L. Carpenter, M. Riparbelli, L. Lehmann, M.K. Gatt, N. Carmo, F. Balloux, G. Callaini, and D.M. Glover. 2005. SAK/PLK4 is required for centriole duplication and flagella development. Curr Biol. 15:2199-2207.

Bobinnec, Y., A. Khodjakov, L. M. Mir, C. L. Rieder, B. Edde and M. Bornens (1998). "Centriole disassembly in vivo and its effect on centrosome structure and function in vertebrate cells." J Cell Biol **143**(6): 1575-1589.

Bobinnec, Y., M. Moudjou, J. P. Fouquet, E. Desbruyeres, B. Edde and M. Bornens (1998). "Glutamylation of centriole and cytoplasmic tubulin in proliferating non-neuronal cells." Cell Motil Cytoskeleton **39**(3): 223-232.

Bornens, M. (2002). "Centrosome composition and microtubule anchoring mechanisms." Curr Opin Cell Biol **14**(1): 25-34.

Boveri, T. (2008). "Concerning the origin of malignant tumours by Theodor Boveri. Translated and annotated by Henry Harris." J Cell Sci **121 Suppl 1**: 1-84.

Brinkley, B. R. (2001). "Managing the centrosome numbers game: from chaos to stability in cancer cell division." Trends Cell Biol **11**(1): 18-21.

Brockerhoff, S. E. and J. M. Fadool (2011). "Genetics of photoreceptor degeneration and regeneration in zebrafish." Cell Mol Life Sci **68**(4): 651-659.

Braun, D.A., and F. Hildebrandt. 2017. Ciliopathies. Cold Spring Harbor perspectives in biology. 9.

Brown, N. J., M. Marjanovic, J. Luders, T. H. Stracker and V. Costanzo (2013). "Cep63 and cep152 cooperate to ensure centriole duplication." PLoS One **8**(7): e69986.

Carvalho-Santos, Z., P. Machado, I. Alvarez-Martins, S.M. Gouveia, S.C. Jana, P. Duarte, T. Amado, P. Branco, M.C. Freitas, S.T. Silva, C. Antony, T.M. Bandeiras, and M. Bettencourt-Dias. 2012. BLD10/CEP135 is a microtubule-associated protein that controls the formation of the flagellum central microtubule pair. Dev Cell. 23:412-424.

Chang, B., H. Khanna, N. Hawes, D. Jimeno, S. He, C. Lillo, S. K. Parapuram, H. Cheng, A. Scott, R. E. Hurd, J. A. Sayer, E. A. Otto, M. Attanasio, J. F. O'Toole, G. Jin, C. Shou, F. Hildebrandt, D. S. Williams, J. R. Heckenlively and A. Swaroop (2006). "In-frame deletion in a novel centrosomal/ciliary protein CEP290/NPHP6 perturbs its interaction with RPGR and results in early-onset retinal degeneration in the rd16 mouse." Hum Mol Genet **15**(11): 1847-1857.

Cheeseman, I. M., T. Hori, T. Fukagawa and A. Desai (2008). "KNL1 and the CENP-H/I/K complex coordinately direct kinetochore assembly in vertebrates." Mol Biol Cell **19**(2): 587-594.

APPENDIX

Christensen, S. T., C. A. Clement, P. Satir and L. B. Pedersen (2012). "Primary cilia and coordination of receptor tyrosine kinase (RTK) signalling." J Pathol **226**(2): 172-184.

Cizmecioglu, O., M. Arnold, R. Bahtz, F. Settele, L. Ehret, U. Haselmann-Weiss, C. Antony, and I. Hoffmann. 2010. Cep152 acts as a scaffold for recruitment of Plk4 and CPAP to the centrosome. J Cell Biol. 191:731-739.

Comartin, D., G. D. Gupta, E. Fussner, E. Coyaud, M. Hasegan, M. Archinti, S. W. Cheung, D. Pinchev, S. Lawo, B. Raught, D. P. Bazett-Jones, J. Luders and L. Pelletier (2013). "CEP120 and SPICE1 cooperate with CPAP in centriole elongation." Curr Biol **23**(14): 1360-1366.

Conduit, P. T., Z. Feng, J. H. Richens, J. Baumbach, A. Wainman, S. D. Bakshi, J. Dobbelaere, S. Johnson, S. M. Lea and J. W. Raff (2014). "The centrosome-specific phosphorylation of Cnn by Polo/Plk1 drives Cnn scaffold assembly and centrosome maturation." Dev Cell **28**(6): 659-669.

Conduit, P. T., A. Wainman and J. W. Raff (2015). "Centrosome function and assembly in animal cells." Nat Rev Mol Cell Biol **16**(10): 611-624.

Conkar, D., E. Culfa, E. Odabasi, N. Rauniyar, J. R. Yates, 3rd and E. N. Firat-Karalar (2017). "The centriolar satellite protein CCDC66 interacts with CEP290 and functions in cilium formation and trafficking." J Cell Sci **130**(8): 1450-1462.

Croxatto, H. B. and M. E. Ortiz (1975). "Egg transport in the fallopian tube." Gynecol Invest **6**(3-4): 215-225.

Cunha-Ferreira, I., I. Bento, A. Pimenta-Marques, S.C. Jana, M. Lince-Faria, P. Duarte, J. Borrego-Pinto, S. Gilberto, T. Amado, D. Brito, A. Rodrigues-Martins, J. Debski, N. Dzhindzhev, and M. Bettencourt-Dias. 2013. Regulation of autophosphorylation controls PLK4 self-destruction and centriole number. Curr Biol. 23:2245-2254.

Dammermann, A., T. Muller-Reichert, L. Pelletier, B. Habermann, A. Desai, and K. Oegema. 2004. Centriole assembly requires both centriolar and pericentriolar material proteins. Developmental Cell. 7:815-829.

Datta, S. R., A. McQuillin, M. Rizig, E. Blaveri, S. Thirumalai, G. Kalsi, J. Lawrence, N. J. Bass, V. Puri, K. Choudhury, J. Pimm, C. Crombie, G. Fraser, N. Walker, D. Curtis, M. Zvelebil, A. Pereira, R. Kandaswamy, D. St Clair and H. M. Gurling (2010). "A threonine to isoleucine missense mutation in the pericentriolar material 1 gene is strongly associated with schizophrenia." Mol Psychiatry **15**(6): 615-628.

Delattre, M., S. Leidel, K. Wani, K. Baumer, J. Bamat, H. Schnabel, R. Feichtinger, R. Schnabel, and P. Gonczy. 2004. Centriolar SAS-5 is required for centrosome duplication in C-elegans. Nature Cell Biology. 6:656-664.

Doxsey, S. (2001). "Re-evaluating centrosome function." Nat Rev Mol Cell Biol **2**(9): 688-698.

Dzhindzhev, N.S., G. Tzolovsky, Z. Lipinszki, M. Abdelaziz, J. Debski, M. Dadlez, and D.M. Glover. 2017. Two-step phosphorylation of Ana2 by Plk4 is required for the sequential loading of Ana2 and Sas6 to initiate procentriole formation. Open Biology. 7.

Dzhindzhev, N.S., Q.D. Yu, K. Weiskopf, G. Tzolovsky, I. Cunha-Ferreira, M. Riparbelli, A. Rodrigues-Martins, M. Bettencourt-Dias, G. Callaini, and D.M. Glover. 2010. Asterless is a scaffold for the onset of centriole assembly. Nature. 467:714-718

Falcon-Urrutia, P., C. M. Carrasco, P. Lois, V. Palma and A. D. Roth (2015). "Shh Signaling through the Primary Cilium Modulates Rat Oligodendrocyte Differentiation." PLoS One **10**(7): e0133567.

Faubel, R., C. Westendorf, E. Bodenschatz and G. Eichele (2016). "Cilia-based flow network in the brain ventricles." Science **353**(6295): 176-178.

Firat-Karalar, E. N., N. Rauniyar, J. R. Yates, 3rd and T. Stearns (2014). "Proximity interactions among centrosome components identify regulators of centriole duplication." Curr Biol **24**(6): 664-670.

Firat-Karalar, E.N., and T. Stearns. 2014. The centriole duplication cycle. Philos Trans R Soc Lond B Biol Sci. 369.

Floriot, S., C. Vesque, S. Rodriguez, F. Bourgain-Guglielmetti, A. Karaiskou, M. Gautier, A. Duchesne, S. Barbey, S. Fritz, A. Vasilescu, M. Bertaud, M. Moudjou, S. Halliez, V. Cormier-Daire, J. E. Hokayem, E. A. Nigg, L. Manciaux, R. Guatteo, N. Cesbron, G. Toutirais, A. Eggen, S. Schneider-Maunoury, D. Boichard, J. Sobczak-Thepot and L. Schibler (2015). "C-Nap1 mutation affects centriole cohesion and is associated with a Seckel-like syndrome in cattle." Nat Commun **6**: 6894.

Friedlander, M. and J. Wahrman (1970). "The spindle as a basal body distributor. A study in the meiosis of the male silkworm moth, Bombyx mori." J Cell Sci **7**(1): 65-89.

Fry, A. M., T. Mayor, P. Meraldi, Y. D. Stierhof, K. Tanaka and E. A. Nigg (1998). "C-Nap1, a novel centrosomal coiled-coil protein and candidate substrate of the cell cycle-regulated protein kinase Nek2." J Cell Biol **141**(7): 1563-1574.

Fu, W., P. Asp, B. Canter and B. D. Dynlacht (2014). "Primary cilia control hedgehog signaling during muscle differentiation and are deregulated in rhabdomyosarcoma." Proc Natl Acad Sci U S A **111**(25): 9151-9156.

Gabriel, E., A. Ramani, U. Karow, M. Gottardo, K. Natarajan, L. M. Gooi, G. Goranci-Buzhala, O. Krut, F. Peters, M. Nikolic, S. Kuivanen, E. Korhonen, T. Smura, O. Vapalahti, A. Papantonis, J. Schmidt-Chanasit, M. Riparbelli, G. Callaini, M. Kronke, O. Utermohlen and J. Gopalakrishnan (2017). "Recent Zika Virus Isolates Induce Premature Differentiation of Neural Progenitors in Human Brain Organoids." Cell Stem Cell **20**(3): 397-406 e395.

Ganem, N. J., S. A. Godinho and D. Pellman (2009). "A mechanism linking extra centrosomes to chromosomal instability." Nature **460**(7252): 278-282.

Ganem, N. J. and D. Pellman (2012). "Linking abnormal mitosis to the acquisition of DNA damage." J Cell Biol **199**(6): 871-881.

Ganem, N. J., Z. Storchova and D. Pellman (2007). "Tetraploidy, aneuploidy and cancer." Curr Opin Genet Dev **17**(2): 157-162.

Ganesan, S., A. T. Comstock and U. S. Sajjan (2013). "Barrier function of airway tract epithelium." Tissue Barriers **1**(4): e24997.

Ganier, O., Schnerch, D., & Nigg, E. A. (2018). Structural centrosome aberrations sensitize polarized epithelia to basal cell extrusion. Open biology, 8(6), 180044.

Ganier, O., D. Schnerch, P. Oertle, R.Y. Lim, M. Plodinec, and E.A. Nigg. 2018b. Structural centrosome aberrations promote non-cell-autonomous invasiveness. EMBO J. 37.

Gheiratmand, L., Coyaud, E., Gupta, G. D., Laurent, E. M., Hasegan, M., Prosser, S. L., … Pelletier, L. (2019). Spatial and proteomic profiling reveals centrosome-independent features of centriolar satellites. The EMBO journal, 38(14), e101109.

Godinho, S.A., R. Picone, M. Burute, R. Dagher, Y. Su, C.T. Leung, K. Polyak, J.S. Brugge, M. Thery, and D. Pellman. 2014. Oncogene-like induction of cellular invasion from centrosome amplification. Nature. 510:167-171.

Goncalves, J. and L. Pelletier (2017). "The Ciliary Transition Zone: Finding the Pieces and Assembling the Gate." Mol Cells **40**(4): 243-253.

Gonczy, P. 2012. Towards a molecular architecture of centriole assembly. Nat Rev Mol Cell Biol. 13:425-435

Gorgidze, L. A. and I. A. Vorobjev (1995). "Centrosome and microtubules behavior in the cytoplasts." J Submicrosc Cytol Pathol **27**(3): 381-389.

Gould, R. R. and G. G. Borisy (1977). "The pericentriolar material in Chinese hamster ovary cells nucleates microtubule formation." J Cell Biol **73**(3): 601-615.

Guderian, G., J. Westendorf, A. Uldschmid, and E.A. Nigg. 2010. Plk4 trans-autophosphorylation regulates centriole number by controlling betaTrCP-mediated degradation. J Cell Sci. 123:2163-2169.

Guichard, P., V. Hachet, N. Majubu, A. Neves, D. Demurtas, N. Olieric, I. Fluckiger, A. Yamada, K. Kihara, Y. Nishida, S. Moriya, M. O. Steinmetz, Y. Hongoh and P. Gonczy (2013). "Native architecture of the centriole proximal region reveals features underlying its 9-fold radial symmetry." Curr Biol **23**(17): 1620-1628.

Gupta, G.D., E. Coyaud, J. Goncalves, B.A. Mojarad, Y. Liu, Q. Wu, L. Gheiratmand, D. Comartin, J.M. Tkach, S.W. Cheung, M. Bashkurov, M.

Habedanck, R., Y.D. Stierhof, C.J. Wilkinson, and E.A. Nigg. 2005. The Polo kinase Plk4 functions in centriole duplication. Nat Cell Biol. 7:1140-1146.

Hall, E. A., M. Keighren, M. J. Ford, T. Davey, A. P. Jarman, L. B. Smith, I. J. Jackson and P. Mill (2013). "Acute versus chronic loss of mammalian Azi1/Cep131 results in distinct ciliary phenotypes." PLoS Genet **9**(12): e1003928.

Hannak, E., M. Kirkham, A. A. Hyman and K. Oegema (2001). "Aurora-A kinase is required for centrosome maturation in Caenorhabditis elegans." J Cell Biol **155**(7): 1109-1116.

Harashima, H., N. Dissmeyer, and A. Schnittger. 2013. "Cell cycle control across the eukaryotic kingdom." Trends Cell Biol. **23**(7): p. 345-56.

Hatch, E.M., A. Kulukian, A.J. Holland, D.W. Cleveland, and T. Stearns. 2010. Cep152 interacts with Plk4 and is required for centriole duplication. J Cell Biol. 191:721-729.

He, R., N. Huang, Y. Bao, H. Zhou, J. Teng and J. Chen (2013). "LRRC45 is a centrosome linker component required for centrosome cohesion." Cell Rep **4**(6): 1100-1107.

Heydeck, W., L. Fievet, E.E. Davis, and N. Katsanis. 2018. The complexity of the cilium: spatiotemporal diversity of an ancient organelle. Curr Opin Cell Biol. 55:139-149.

Hilbert, M., A. Noga, D. Frey, V. Hamel, P. Guichard, S. H. Kraatz, M. Pfreundschuh, S. Hosner, I. Fluckiger, R. Jaussi, M. M. Wieser, K. M. Thieltges, X. Deupi, D. J. Muller, R. A. Kammerer, P. Gonczy, M. Hirono and M. O. Steinmetz (2016). "SAS-6 engineering reveals interdependence between cartwheel and microtubules in determining centriole architecture." Nat Cell Biol **18**(4): 393-403.

Hinchcliffe, E. H., F. J. Miller, M. Cham, A. Khodjakov and G. Sluder (2001). "Requirement of a centrosomal activity for cell cycle progression through G1 into S phase." Science **291**(5508): 1547-1550.

Hoh, R. A., T. R. Stowe, E. Turk and T. Stearns (2012). "Transcriptional program of ciliated epithelial cells reveals new cilium and centrosome components and links to human disease." PLoS One **7**(12): e52166.

Holland, A.J., D. Fachinetti, Q. Zhu, M. Bauer, I.M. Verma, E.A. Nigg, and D.W. Cleveland. 2012. The autoregulated instability of Polo-like kinase 4 limits centrosome duplication to once per cell cycle. Genes Dev. 26:2684-2689.

Hong, D. H., B. Pawlyk, M. Sokolov, K. J. Strissel, J. Yang, B. Tulloch, A. F. Wright, V. Y. Arshavsky and T. Li (2003). "RPGR isoforms in photoreceptor connecting cilia and the transitional zone of motile cilia." Invest Ophthalmol Vis Sci **44**(6): 2413-2421.

Hopkins, M., J.J. Tyson, and B. Novak. 2017. Cell-cycle transitions: a common role for stoichiometric inhibitors. Mol Biol Cell, 2017. **28**(23): p. 3437-3446.

Hori, A., and T. Toda. 2017. Regulation of centriolar satellite integrity and its physiology. Cell Mol Life Sci. 74:213-229.

Hsiao, K. Y., Y. C. Lin, S. K. Gupta, N. Chang, L. Yen, H. S. Sun and S. J. Tsai (2017). "Noncoding Effects of Circular RNA CCDC66 Promote Colon Cancer Growth and Metastasis." Cancer Res **77**(9): 2339-2350.

Hu, H., Y. Liu, Q. Zhou, S. Siegel and Z. Li (2015). "The Centriole Cartwheel Protein SAS-6 in Trypanosoma brucei Is Required for Probasal Body Biogenesis and Flagellum Assembly." Eukaryot Cell **14**(9): 898-907.

Hueschen, C.L., S.J. Kenny, K. Xu, and S. Dumont. 2017. NuMA recruits dynein activity to microtubule minus-ends at mitosis. eLife. 6.

Huang, N., Y. Xia, D. Zhang, S. Wang, Y. Bao, R. He, J. Teng and J. Chen (2017). "Hierarchical assembly of centriole subdistal appendages via centrosome binding proteins CCDC120 and CCDC68." Nat Commun **8**: 15057.

Huangfu, D., A. Liu, A. S. Rakeman, N. S. Murcia, L. Niswander and K. V. Anderson (2003). "Hedgehog signalling in the mouse requires intraflagellar transport proteins." Nature **426**(6962): 83-87.

Hussain, M. S., S. M. Baig, S. Neumann, G. Nurnberg, M. Farooq, I. Ahmad, T. Alef, H. C. Hennies, M. Technau, J. Altmuller, P. Frommolt, H. Thiele, A. A. Noegel and P. Nurnberg (2012). "A truncating mutation of CEP135 causes primary microcephaly and disturbed centrosomal function." Am J Hum Genet **90**(5): 871-878.

Hsu, W.B., L.Y. Hung, C.J. Tang, C.L. Su, Y. Chang, and T.K. Tang. 2008. Functional characterization of the microtubule-binding and -destabilizing domains of CPAP and d-SAS-4. Exp Cell Res. 314:2591-2602.

Janke, C. and J. C. Bulinski (2011). "Post-translational regulation of the microtubule cytoskeleton: mechanisms and functions." Nat Rev Mol Cell Biol **12**(12): 773-786.

Jayaraman, D., B.I. Bae, and C.A. Walsh. 2018. The Genetics of Primary Microcephaly. Annu Rev Genomics Hum Genet. 19:177-200.

Keller, D., M. Orpinell, N. Olivier, M. Wachsmuth, R. Mahen, R. Wyss, V. Hachet, J. Ellenberg, S. Manley and P. Gonczy (2014). "Mechanisms of HsSAS-6 assembly promoting centriole formation in human cells." J Cell Biol **204**(5): 697-712.

Kemp, C.A., K.R. Kopish, P. Zipperlen, J. Ahringer, and K.F. O'Connell. 2004. Centrosome maturation and duplication in C. elegans require the coiled-coil protein SPD-2. Dev Cell. 6:511-523.

Khan, A. O., B. S. Budde, P. Nurnberg, A. Kawalia, S. Lenzner and H. J. Bolz (2018). "Genome-wide linkage and sequence analysis challenge CCDC66 as a human retinal dystrophy candidate gene and support a distinct NMNAT1-related fundus phenotype." Clin Genet **93**(1): 149-154.

Khodjakov, A., R. W. Cole, B. R. Oakley and C. L. Rieder (2000). "Centrosome-independent mitotic spindle formation in vertebrates." Curr Biol **10**(2): 59-67.

Kilmartin, J. V. (2003). "Sfi1p has conserved centrin-binding sites and an essential function in budding yeast spindle pole body duplication." J Cell Biol **162**(7): 1211-1221.

Kim, J., S. R. Krishnaswami and J. G. Gleeson (2008). "CEP290 interacts with the centriolar satellite component PCM-1 and is required for Rab8 localization to the primary cilium." Hum Mol Genet **17**(23): 3796-3805.

Kim, T. S., J. E. Park, A. Shukla, S. Choi, R. N. Murugan, J. H. Lee, M. Ahn, K. Rhee, J. K. Bang, B. Y. Kim, J. Loncarek, R. L. Erikson and K. S. Lee (2013). "Hierarchical recruitment of Plk4 and regulation of centriole biogenesis by two centrosomal scaffolds, Cep192 and Cep152." Proc Natl Acad Sci U S A **110**(50): E4849-4857.

Kirkham, M., T. Muller-Reichert, K. Oegema, S. Grill and A. A. Hyman (2003). "SAS-4 is a C. elegans centriolar protein that controls centrosome size." Cell **112**(4): 575-587.

Kitagawa, D., I. Vakonakis, N. Olieric, M. Hilbert, D. Keller, V. Olieric, M. Bortfeld, M.C. Erat, I. Fluckiger, P. Gonczy, and M.O. Steinmetz. 2011. Structural Basis of the 9-Fold Symmetry of Centrioles. Cell. 144:364-375.

Klebba, J.E., D.W. Buster, A.L. Nguyen, S. Swatkoski, M. Gucek, N.M. Rusan, and G.C. Rogers. 2013. Polo-like kinase 4 autodestructs by generating its Slimb-binding phosphodegron. Curr Biol. 23:2255-2261.

Kodani, A., T.W. Yu, J.R. Johnson, D. Jayaraman, T.L. Johnson, L. Al-Gazali, L. Sztriha, J.N. Partlow, H. Kim, A.L. Krup, A. Dammermann, N.J. Krogan, C.A. Walsh, and J.F. Reiter. 2015. Centriolar satellites assemble centrosomal microcephaly proteins to recruit CDK2 and promote centriole duplication. eLife. 4.

Kollman, J. M., A. Merdes, L. Mourey and D. A. Agard (2011). "Microtubule nucleation by gamma-tubulin complexes." Nat Rev Mol Cell Biol **12**(11): 709-721.

Kubo, A. and S. Tsukita (2003). "Non-membranous granular organelle consisting of PCM-1: subcellular distribution and cell-cycle-dependent assembly/disassembly." J Cell Sci **116**(Pt 5): 919-928.

Kuijpers, M. and C. C. Hoogenraad (2011). "Centrosomes, microtubules and neuronal development." Mol Cell Neurosci **48**(4): 349-358.

Kunimoto, K., Y. Yamazaki, T. Nishida, K. Shinohara, H. Ishikawa, T. Hasegawa, T. Okanoue, H. Hamada, T. Noda, A. Tamura, S. Tsukita and S. Tsukita (2012). "Coordinated ciliary beating requires Odf2-mediated polarization of basal bodies via basal feet." Cell **148**(1-2): 189-200.

Kushner, E. J., L. S. Ferro, J. Y. Liu, J. R. Durrant, S. L. Rogers, A. C. Dudley and V. L. Bautch (2014). "Excess centrosomes disrupt endothelial cell migration via centrosome scattering." J Cell Biol **206**(2): 257-272.

Kwon, M., S. A. Godinho, N. S. Chandhok, N. J. Ganem, A. Azioune, M. Thery and D. Pellman (2008). "Mechanisms to suppress multipolar divisions in cancer cells with extra centrosomes." Genes Dev **22**(16): 2189-2203.

Lane, H. A. and E. A. Nigg (1996). "Antibody microinjection reveals an essential role for human polo-like kinase 1 (Plk1) in the functional maturation of mitotic centrosomes." J Cell Biol **135**(6 Pt 2): 1701-1713.

Lawo, S., M. Hasegan, G. D. Gupta and L. Pelletier (2012). "Subdiffraction imaging of centrosomes reveals higher-order organizational features of pericentriolar material." Nat Cell Biol **14**(11): 1148-1158.

Lee, K. and K. Rhee (2011). "PLK1 phosphorylation of pericentrin initiates centrosome maturation at the onset of mitosis." J Cell Biol **195**(7): 1093-1101.

Leidel, S., M. Delattre, L. Cerutti, K. Baumer and P. Gonczy (2005). "SAS-6 defines a protein family required for centrosome duplication in C. elegans and in human cells." Nat Cell Biol **7**(2): 115-125.

Lemullois, M., E. Boisvieux-Ulrich, M. C. Laine, B. Chailley and D. Sandoz (1988). "Development and functions of the cytoskeleton during ciliogenesis in metazoa." Biol Cell **63**(2): 195-208.

Levine, M. S., B. Bakker, B. Boeckx, J. Moyett, J. Lu, B. Vitre, D. C. Spierings, P. M. Lansdorp, D. W. Cleveland, D. Lambrechts, F. Foijer and A. J. Holland (2017). "Centrosome Amplification Is Sufficient to Promote Spontaneous Tumorigenesis in Mammals." Dev Cell **40**(3): 313-322 e315.

Li, S., J. J. Fernandez, W. F. Marshall and D. A. Agard (2012). "Three-dimensional structure of basal body triplet revealed by electron cryo-tomography." EMBO J **31**(3): 552-562.

Lin, Y.C., C.W. Chang, W.B. Hsu, C.J.C. Tang, N. Lin, E.J. Chou, C.T. Wu, and T.K. Tang. 2013a. Human microcephaly protein CEP135 binds to hSAS-6 and CPAP, and is required for centriole assembly. Embo Journal. 32:1141-1154.

Lin, Y.N., C.T. Wu, Y.C. Lin, W.B. Hsu, C.J. Tang, C.W. Chang, and T.K. Tang. 2013b. CEP120 interacts with CPAP and positively regulates centriole elongation. J Cell Biol. 202:211-219.

Liu, Q., J. Zhou, S. P. Daiger, D. B. Farber, J. R. Heckenlively, J. E. Smith, L. S. Sullivan, J. Zuo, A. H. Milam and E. A. Pierce (2002). "Identification and subcellular localization of the RP1 protein in human and mouse photoreceptors." Invest Ophthalmol Vis Sci **43**(1): 22-32.

Lloyd, C. W. (1989). "The plant cytoskeleton." Curr Opin Cell Biol **1**(1): 30-35.

Lopes, C.A.M., M. Mesquita, A.I. Cunha, J. Cardoso, S. Carapeta, C. Laranjeira, A.E. Pinto, J.B. Pereira-Leal, A. Dias-Pereira, M. Bettencourt-Dias, and P. Chaves. 2018. Centrosome amplification arises before neoplasia and increases upon p53 loss in tumorigenesis. J Cell Biol. 217:2353-2363.

Lukinavicius, G., D. Lavogina, M. Orpinell, K. Umezawa, L. Reymond, N. Garin, P. Gonczy and K. Johnsson (2013). "Selective chemical crosslinking reveals a Cep57-Cep63-Cep152 centrosomal complex." Curr Biol **23**(3): 265-270.

Mana-Capelli, S., R. Graf and D. A. Larochelle (2009). "Dictyostelium discoideum CenB is a bona fide centrin essential for nuclear architecture and centrosome stability." Eukaryot Cell **8**(8): 1106-1117.

Mardin, B. R., C. Lange, J. E. Baxter, T. Hardy, S. R. Scholz, A. M. Fry and E. Schiebel (2010). "Components of the Hippo pathway cooperate with Nek2 kinase to regulate centrosome disjunction." Nat Cell Biol **12**(12): 1166-1176.

Mardin, B. R. and E. Schiebel (2012). "Breaking the ties that bind: new advances in centrosome biology." J Cell Biol **197**(1): 11-18.

Marjanovic, M., C. Sanchez-Huertas, B. Terre, R. Gomez, J.F. Scheel, S. Pacheco, P.A. Knobel, A. Martinez-Marchal, S. Aivio, L. Palenzuela, U. Wolfrum, P.J. McKinnon, J.A. Suja, I. Roig, V. Costanzo, J. Luders, and T.H. Stracker. 2015. CEP63 deficiency promotes p53-dependent microcephaly and reveals a role for the centrosome in meiotic recombination. Nat Commun. 6:7676.

Marshall, W. F. (2008). "Basal bodies platforms for building cilia." Curr Top Dev Biol **85**: 1-22.

Marshall, W. F. and S. Nonaka (2006). "Cilia: tuning in to the cell's antenna." Curr Biol **16**(15): R604-614.

Marszalek, J. R., X. Liu, E. A. Roberts, D. Chui, J. D. Marth, D. S. Williams and L. S. Goldstein (2000). "Genetic evidence for selective transport of opsin and arrestin by kinesin-II in mammalian photoreceptors." Cell **102**(2): 175-187.

Marthiens, V., M. A. Rujano, C. Pennetier, S. Tessier, P. Paul-Gilloteaux and R. Basto (2013). "Centrosome amplification causes microcephaly." Nat Cell Biol **15**(7): 731-740.

Mayor, T., Y. D. Stierhof, K. Tanaka, A. M. Fry and E. A. Nigg (2000). "The centrosomal protein C-Nap1 is required for cell cycle-regulated centrosome cohesion." J Cell Biol **151**(4): 837-846.

McLamarrah, T.A., D.W. Buster, B.J. Galletta, C.J. Boese, J.M. Ryniawec, N.A. Hollingsworth, A.E. Byrnes, C.W. Brownlee, K.C. Slep, N.M. Rusan, and G.C. Rogers. 2018. An ordered pattern of Ana2 phosphorylation by Plk4 is required for centriole assembly. Journal of Cell Biology. 217:1217-1231

Mennella, V., B. Keszthelyi, K. L. McDonald, B. Chhun, F. Kan, G. C. Rogers, B. Huang and D. A. Agard (2012). "Subdiffraction-resolution fluorescence microscopy reveals a domain of the centrosome critical for pericentriolar material organization." Nat Cell Biol **14**(11): 1159-1168.

Mitchell, D. R. (2007). "The evolution of eukaryotic cilia and flagella as motile and sensory organelles." Adv Exp Med Biol **607**: 130-140.

Nakazawa, Y., M. Hiraki, R. Kamiya, and M. Hirono. 2007. SAS-6 is a cartwheel protein that establishes the 9-fold symmetry of the centriole. Current Biology. 17:2169-2174.

Nirono (2007). "SAS-6 is a cartwheel protein that establishes the 9-fold symmetry of the centriole." Curr Biol **17**(24): 2169-2174.

Nigg, E. A. (2002). "Centrosome aberrations: cause or consequence of cancer progression?" Nat Rev Cancer **2**(11): 815-825.

Nigg, E. A. (2007). "Centrosome duplication: of rules and licenses." Trends Cell Biol **17**(5): 215-221.

Nigg, E.A., and A.J. Holland. 2018. Once and only once: mechanisms of centriole duplication and their deregulation in disease. Nat Rev Mol Cell Biol. 19:297-312.

Nigg, E.A., and J.W. Raff. 2009. Centrioles, centrosomes, and cilia in health and disease. Cell. 139:663-678.

Nigg, E. A. and T. Stearns (2011). "The centrosome cycle: Centriole biogenesis, duplication and inherent asymmetries." Nat Cell Biol **13**(10): 1154-1160.

Nonaka, S., Y. Tanaka, Y. Okada, S. Takeda, A. Harada, Y. Kanai, M. Kido and N. Hirokawa (1998). "Randomization of left-right asymmetry due to loss of nodal cilia generating leftward flow of extraembryonic fluid in mice lacking KIF3B motor protein." Cell **95**(6): 829-837.

Norbury, C. and P. Nurse, Animal cell cycles and their control. Annu Rev Biochem, 1992. 61: p. 441-70.

O'Connell, K.F., C. Caron, K.R. Kopish, D.D. Hurd, K.J. Kemphues, Y.J. Li, and J.G. White. 2001. The C-elegans zyg-1 gene encodes a regulator of centrosome duplication with distinct maternal and paternal roles in the embryo. Cell. 105:547-558.

O'Neill, R.S., T.A. Schoborg, and N.M. Rusan. 2018. Same but different: pleiotropy in centrosome-related microcephaly. Molecular Biology of the Cell. 29:241-246.

Odabasi, E., S. Gul, I.H. Kavakli, and E.N. Firat-Karalar. 2019. Centriolar satellites are required for efficient ciliogenesis and ciliary content regulation. EMBO Rep.

Ohta, T., R. Essner, J.H. Ryu, R.E. Palazzo, Y. Uetake, and R. Kuriyama. 2002. Characterization of Cep135, a novel coiled-coil centrosomal protein involved in microtubule organization in mammalian cells. Journal of Cell Biology. 156:87-99.

Palazzo, R. E., J. M. Vogel, B. J. Schnackenberg, D. R. Hull and X. Wu (2000). "Centrosome maturation." Curr Top Dev Biol **49**: 449-470.

Paz, J., and J. Luders. 2018. Microtubule-Organizing Centers: Towards a Minimal Parts List. Trends Cell Biol. 28:176-187.

Pazour, G. J., S. A. Baker, J. A. Deane, D. G. Cole, B. L. Dickert, J. L. Rosenbaum, G. B. Witman and J. C. Besharse (2002). "The intraflagellar transport protein, IFT88, is essential for vertebrate photoreceptor assembly and maintenance." J Cell Biol **157**(1): 103-113.

Pazour, G. J., B. L. Dickert, Y. Vucica, E. S. Seeley, J. L. Rosenbaum, G. B. Witman and D. G. Cole (2000). "Chlamydomonas IFT88 and its mouse homologue, polycystic kidney disease gene tg737, are required for assembly of cilia and flagella." J Cell Biol **151**(3): 709-718.

Pearson, C. G., T. H. Giddings, Jr. and M. Winey (2009). "Basal body components exhibit differential protein dynamics during nascent basal body assembly." Mol Biol Cell **20**(3): 904-914.

Pennekamp, P., T. Menchen, B. Dworniczak and H. Hamada (2015). "Situs inversus and ciliary abnormalities: 20 years later, what is the connection?" Cilia **4**(1): 1.

Pelletier, L., N. Ozlu, E. Hannak, C. Cowan, B. Habermann, M. Ruer, T. Muller-Reichert, and A.A. Hyman. 2004a. The Caenorhabditis elegans centrosomal protein SPD-2 is required for both pericentriolar material recruitment and centriole duplication. Current Biology. 14:863-873.

Pelletier, L., N. Ozlu, E. Hannak, C. Cowan, B. Habermann, M. Ruer, T. Muller-Reichert, and A.A. Hyman. 2004b. The Caenorhabditis elegans centrosomal protein SPD-2 is required for both pericentriolar material recruitment and centriole duplication. Curr Biol. 14:863-873.

Piehl, M., U. S. Tulu, P. Wadsworth and L. Cassimeris (2004). "Centrosome maturation: measurement of microtubule nucleation throughout the cell cycle by using GFP-tagged EB1." Proc Natl Acad Sci U S A **101**(6): 1584-1588.

Raidt, J., C. Werner, T. Menchen, G. W. Dougherty, H. Olbrich, N. T. Loges, R. Schmitz, P. Pennekamp and H. Omran (2015). "Ciliary function and motor protein composition of human fallopian tubes." Hum Reprod **30**(12): 2871-2880.

Reiter, J.F., and M.R. Leroux. 2017. Genes and molecular pathways underpinning ciliopathies. Nat Rev Mol Cell Biol. 18:533-547.

Rieder, C. L., S. Faruki and A. Khodjakov (2001). "The centrosome in vertebrates: more than a microtubule-organizing center." Trends Cell Biol **11**(10): 413-419.

Ringo, D. L. (1967). "Flagellar motion and fine structure of the flagellar apparatus in Chlamydomonas." J Cell Biol **33**(3): 543-571.

Riparbelli, M. G., R. Dallai and G. Callaini (2010). "The insect centriole: A land of discovery." Tissue Cell **42**(2): 69-80.

Sanchez, I. and B. D. Dynlacht (2016). "Cilium assembly and disassembly." Nat Cell Biol **18**(7): 711-717.

Satir, P. and S. T. Christensen (2007). "Overview of structure and function of mammalian cilia." Annu Rev Physiol **69**: 377-400.

Satir, P., L. B. Pedersen and S. T. Christensen (2010). "The primary cilium at a glance." J Cell Sci **123**(Pt 4): 499-503.

Saurin, A.T., et al., 2011 "Aurora B potentiates Mps1 activation to ensure rapid checkpoint establishment at the onset of mitosis." Nat Commun. **2**: p. 316.

Scheer, U. (2014). "Historical roots of centrosome research: discovery of Boveri's microscope slides in Wurzburg." Philos Trans R Soc Lond B Biol Sci **369**(1650).

Schneider, C.A., W.S. Rasband, and K.W. Eliceiri. 2012. NIH Image to ImageJ: 25 years of image analysis. Nat Methods. 9:671-675.

Schmidt, T. I., J. Kleylein-Sohn, J. Westendorf, M. Le Clech, S. B. Lavoie, Y. D. Stierhof and E. A. Nigg (2009). "Control of centriole length by CPAP and CP110." Curr Biol **19**(12): 1005-1011.

Sercin, O., J.C. Larsimont, A.E. Karambelas, V. Marthiens, V. Moers, B. Boeckx, M. Le Mercier, D. Lambrechts, R. Basto, and C. Blanpain. 2016. Transient PLK4 overexpression accelerates tumorigenesis in p53-deficient epidermis. Nat Cell Biol. 18:100-110.

Sharma, A., A. Aher, N. J. Dynes, D. Frey, E. A. Katrukha, R. Jaussi, I. Grigoriev, M. Croisier, R. A. Kammerer, A. Akhmanova, P. Gonczy and M. O. Steinmetz (2016). "Centriolar CPAP/SAS-4 Imparts Slow Processive Microtubule Growth." Dev Cell **37**(4): 362-376.

Silkworth, W.T., I.K. Nardi, L.M. Scholl, and D. Cimini. 2009. Multipolar spindle pole coalescence is a major source of kinetochore mis-attachment and chromosome mis-segregation in cancer cells. PLoS One. 4:e6564.

Singla, V. and J. F. Reiter (2006). "The primary cilium as the cell's antenna: signaling at a sensory organelle." Science **313**(5787): 629-633.

Sir, J.H., A.R. Barr, A.K. Nicholas, O.P. Carvalho, M. Khurshid, A. Sossick, S. Reichelt, C. D'Santos, C.G. Woods, and F. Gergely. 2011. A primary microcephaly protein complex forms a ring around parental centrioles. Nat Genet. **43**:1147-1153

Sivakumar, S. and G.J. Gorbsky. 2015. "Spatiotemporal regulation of the anaphase-promoting complex in mitosis." Nature Reviews Molecular Cell Biology. **16**: p. 82.

Sluder, G. and J. J. Nordberg (2004). "The good, the bad and the ugly: the practical consequences of centrosome amplification." Curr Opin Cell Biol **16**(1): 49-54.

Sonnen, K. F., L. Schermelleh, H. Leonhardt and E. A. Nigg (2012). "3D-structured illumination microscopy provides novel insight into architecture of human centrosomes." Biol Open **1**(10): 965-976.

Spektor, A., W. Y. Tsang, D. Khoo and B. D. Dynlacht (2007). "Cep97 and CP110 suppress a cilia assembly program." Cell **130**(4): 678-690.

Stinchcombe, J. C., L. O. Randzavola, K. L. Angus, J. M. Mantell, P. Verkade and G. M. Griffiths (2015). "Mother Centriole Distal Appendages Mediate Centrosome Docking at the Immunological Synapse and Reveal Mechanistic Parallels with Ciliogenesis." Curr Biol **25**(24): 3239-3244.

Szollosi, D., P. Calarco and R. P. Donahue (1972). "Absence of centrioles in the first and second meiotic spindles of mouse oocytes." J Cell Sci **11**(2): 521-541.

Tanenbaum, M. E. and R. H. Medema (2010). "Mechanisms of centrosome separation and bipolar spindle assembly." Dev Cell **19**(6): 797-806.

Tanos, B. E., H. J. Yang, R. Soni, W. J. Wang, F. P. Macaluso, J. M. Asara and M. F. Tsou (2013). "Centriole distal appendages promote membrane docking, leading to cilia initiation." Genes Dev **27**(2): 163-168.

Tollenaere, M. A., N. Mailand and S. Bekker-Jensen (2015). "Centriolar satellites: key mediators of centrosome functions." Cell Mol Life Sci **72**(1): 11-23.

Tsou, M. F. and T. Stearns (2006). "Controlling centrosome number: licenses and blocks." Curr Opin Cell Biol **18**(1): 74-78.

van Breugel, M., M. Hirono, A. Andreeva, H. Yanagisawa, S. Yamaguchi, Y. Nakazawa, N. Morgner, M. Petrovich, I.O. Ebong, C.V. Robinson, C.M. Johnson, D. Veprintsev, and B. Zuber. 2011. Structures of SAS-6 Suggest Its Organization in Centrioles. Science. 331:1196-1199.

Van de Mark, D., D. Kong, J. Loncarek, and T. Stearns. 2015. MDM1 is a microtubule-binding protein that negatively regulates centriole duplication. Mol Biol Cell. 26:3788-3802.

van Dam, T. J., M. J. Townsend, M. Turk, A. Schlessinger, A. Sali, M. C. Field and M. A. Huynen (2013). "Evolution of modular intraflagellar transport from a coatomer-like progenitor." Proc Natl Acad Sci U S A **110**(17): 6943-6948.

Vermeulen, K., D.R. Van Bockstaele, and Z.N. Berneman. 2003. The cell cycle: a review of regulation, deregulation and therapeutic targets in cancer. Cell Prolif. **36**(3): p. 131-49.

Vitre, B., A. J. Holland, A. Kulukian, O. Shoshani, M. Hirai, Y. Wang, M. Maldonado, T. Cho, J. Boubaker, D. A. Swing, L. Tessarollo, S. M. Evans, E. Fuchs and D. W. Cleveland (2015). "Chronic centrosome amplification without tumorigenesis." Proc Natl Acad Sci U S A **112**(46): E6321-6330.

Wakida, N. M., E. L. Botvinick, J. Lin and M. W. Berns (2010). "An intact centrosome is required for the maintenance of polarization during directional cell migration." PLoS One **5**(12): e15462.

Wang, L., K. Lee, R. Malonis, I. Sanchez, and B.D. Dynlacht. 2016. Tethering of an E3 ligase by PCM1 regulates the abundance of centrosomal KIAA0586/Talpid3 and promotes ciliogenesis. eLife. 5.

Waters, A. M. and P. L. Beales (2011). "Ciliopathies: an expanding disease spectrum." Pediatr Nephrol **26**(7): 1039-1056.

Winey, M. and E. O'Toole (2014). "Centriole structure." Philos Trans R Soc Lond B Biol Sci **369**(1650).

Woodruff, J. B., O. Wueseke and A. A. Hyman (2014). "Pericentriolar material structure and dynamics." Philos Trans R Soc Lond B Biol Sci **369**(1650).

Wu, J., and A. Akhmanova. 2017. Microtubule-Organizing Centers. Annual review of cell and developmental biology. 33:51-75.

Yadav, S., P.J. Verma, and D. Panda. 2014. C-terminal region of MAP7 domain containing protein 3 (MAP7D3) promotes microtubule polymerization by binding at the C-terminal tail of tubulin. PLoS One. 9:e99539.

Yang, J., X. Liu, G. Yue, M. Adamian, O. Bulgakov and T. Li (2002). "Rootletin, a novel coiled-coil protein, is a structural component of the ciliary rootlet." J Cell Biol **159**(3): 431-440.

APPENDIX

Yang, Y. J., A. E. Baltus, R. S. Mathew, E. A. Murphy, G. D. Evrony, D. M. Gonzalez, E. P. Wang, C. A. Marshall-Walker, B. J. Barry, J. Murn, A. Tatarakis, M. A. Mahajan, H. H. Samuels, Y. Shi, J. A. Golden, M. Mahajnah, R. Shenhav and C. A. Walsh (2012). "Microcephaly gene links trithorax and REST/NRSF to control neural stem cell proliferation and differentiation." Cell **151**(5): 1097-1112.

Zach, F., F. Grassmann, T. Langmann, N. Sorusch, U. Wolfrum and H. Stohr (2012). "The retinitis pigmentosa 28 protein FAM161A is a novel ciliary protein involved in intermolecular protein interaction and microtubule association." Hum Mol Genet **21**(21): 4573-4586.

Zariwala, M. A., M. R. Knowles and H. Omran (2007). "Genetic defects in ciliary structure and function." Annu Rev Physiol **69**: 423-450.

Zhao, H., L. Zhu, Y. Zhu, J. Cao, S. Li, Q. Huang, T. Xu, X. Huang, X. Yan and X. Zhu (2013). "The Cep63 paralogue Deup1 enables massive de novo centriole biogenesis for vertebrate multiciliogenesis." Nat Cell Biol **15**(12): 1434-1444.

Zheng, X., A. Ramani, K. Soni, M. Gottardo, S. Zheng, L. Ming Gooi, W. Li, S. Feng, A. Mariappan, A. Wason, P. Widlund, A. Pozniakovsky, I. Poser, H. Deng, G. Ou, M. Riparbelli, C. Giuliano, A. A. Hyman, M. Sattler, J. Gopalakrishnan and H. Li (2016). "Molecular basis for CPAP-tubulin interaction in controlling centriolar and ciliary length." Nat Commun **7**: 11874.

Zybailov, B., A.L. Mosley, M.E. Sardiu, M.K. Coleman, L. Florens, and M.P. Washburn. 2006. Statistical analysis of membrane proteome expression changes in Saccharomyces cerevisiae. J Proteome Res. 5:2339-2347.

APPENDIX

Table 1. Primer sets used to generate truncated forms of CCDC57

Fragment (aa)	Forward Primer (5'-3')	Reverse Primer (5'-3')
1-916 full length	**GGGGACAACTTTGTACAAAAAAGTTGAT** ATGCTGCCACTGGGCTCAGAG	**GGGGACAACTTTGTACAAGAAAGTTGT** TAACTACAACATTATGGACTGA
1-502	**GGGGACAACTTTGTACAAAAAAGTTGAT** ATGCTGCCACTGGGCTCAGAG	**GGGGACAACTTTGTACAAGAAAGTTGT** CTGCCTGAGAAGCATCTGTGC
503-916	**GGGGACAACTTTGTACAAAAAAGTTGAT** GGCACAGATGCTTCTCAGGCAG	**GGGGACAACTTTGTACAAGAAAGTTGT** TAACTACAACATTATGGACTGA
606-916	**GGGGACAACTTTGTACAAAAAAGTTGAT** CCTTTAAAGATGTCCTCACCTCATG	**GGGGACAACTTTGTACAAGAAAGTTGT** TAACTACAACATTATGGACTGA
1-605	**GGGGACAACTTTGTACAAAAAAGTTGAT**	**GGGGACAACTTTGTACAAGAAAGTTGT**

APPENDIX

	ATGCTGCCACTGGGCTCAGAG	GGATCCAACACATCTTCTAGATGC
684-916	**GGGGACAACTTTGTACAAAAAAGTTGAT** GAACCCCTGGAGCCGGCCGCTC	**GGGGACAACTTTGTACAAGAAAGTTGT** TAACTACAACATTATGGACTGA

gateway sequence / annealing sequence